Eyes Wide Open: Ego Proactive Video-LLM for Streaming Video

Yulin Zhang[1] **Cheng Shi**[3] **Yang Wang**[1] **Sibei Yang**[2†]
[1]ShanghaiTech University [2]School of Computer Science and Engineering, Sun Yat-sen University
[3]School of Computing and Data Science, The University of Hong Kong
Project Page: https://zhangyl4.github.io/publications/eyes-wide-open/

Abstract

Envision an AI capable of functioning in human-like settings, moving beyond mere observation to actively understand, anticipate, and proactively respond to unfolding events. Towards this vision, we focus on the innovative task where, *given ego-streaming video input, an assistant proactively answers diverse, evolving questions at the opportune moment, while maintaining synchronized perception and reasoning.* This task embodies three key properties: (1) Proactive Coherence, (2) Just-in-Time Responsiveness, and (3) Synchronized Efficiency. To evaluate and address these properties, we first introduce ESTP-Bench (Ego Streaming Proactive Benchmark) alongside the ESTP-F1 metric—a novel framework designed for their rigorous assessment. Secondly, we propose a comprehensive technical pipeline to enable models to tackle this challenging task. This pipeline comprises: (1) a data engine, (2) a multi-stage training strategy, and (3) a proactive dynamic compression technique. Our proposed model effectively addresses these critical properties while outperforming multiple baselines across diverse online and offline benchmarks.

1 Introduction

Imagine an AI assistant that follows you through your day—assembling furniture, searching for misplaced keys [3, 15], or preparing a meal [46, 44]—not just watching, but understanding, anticipating [54], and responding proactively when needed as events unfold. To function in such human-like settings, where visual input is egocentric and continuously streaming, and user needs shift from moment to moment, the assistant must go beyond passive observation. It should be able to interpret the present, anticipate what comes next, and respond at exactly the right moment, all in real time.

As a first step toward this vision, we narrow our focus to perception and understanding in egocentric streaming video, with a particular emphasis on the following innovative task: ***Given ego-streaming video input, the assistant proactively answers to diverse and evolving questions at the right moment, while seeing and thinking in sync,*** as shown in Fig. 1. This task relies on three key properties:

- Proactive Coherence: handling diverse question types, responding even when answers depend on future visual streams (proactivity), and maintaining contextual consistency across related questions. In ego-streaming scenarios, questions often go beyond the current frame, referencing future events or past observations. As shown in Fig. 1, the segment of the conversation highlighted in green is contextually dependent on the content within the segment highlighted in purple. Such queries require temporal integration of past and present information, followed by proactive answering as relevant visual evidence emerges.
- Just-in-Time Responsiveness: determining when to answer based on visual readiness, neither too soon nor too late, and only when necessary. Responding before enough evidence is available can

†Corresponding author is Sibei Yang.

39th Conference on Neural Information Processing Systems (NeurIPS 2025).

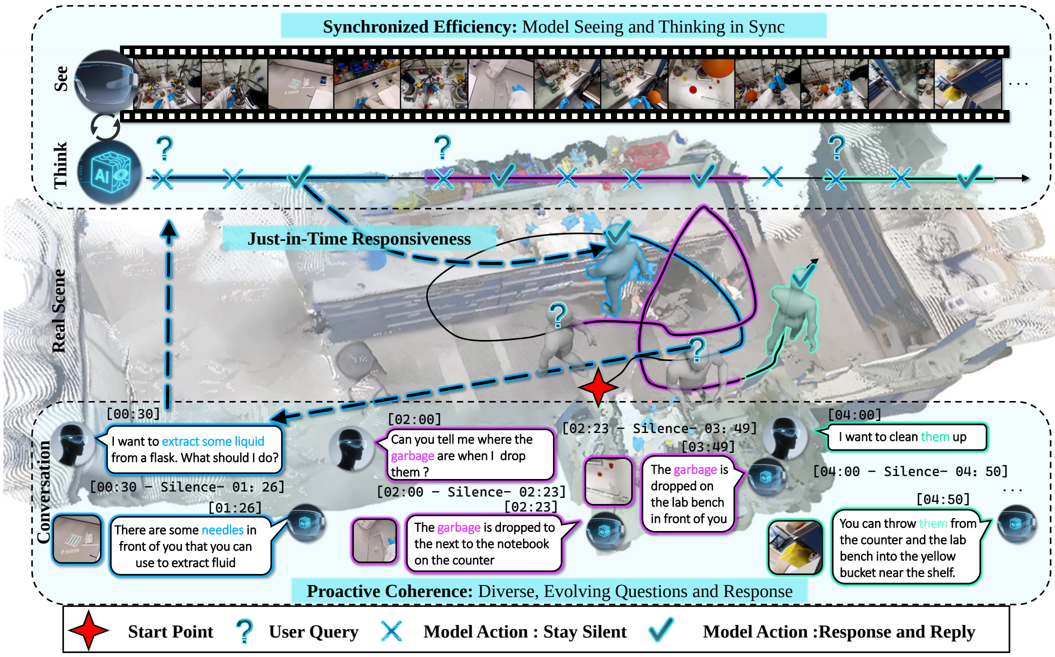

Figure 1: **An illustrative example of the ESTP task.** The figure is structured in three layers: the top layer depicts the model's continuous visual processing and decision-making (*See and Think*), the middle layer shows the real-world egocentric scene with the human's trajectory, and the bottom layer presents the human-model conversation.

lead to mistakes, while answering too late may miss the opportunity to help. Equally important is staying silent when uncertain and avoiding unnecessary repetition. As shown in the blue-highlighted segment of Fig. 1, it is necessary to remain silent until the "face to counter". The assistant must continuously track the evolving visual context and respond at the earliest reliable moment.

- Synchronized Efficiency: ensuring that answering and visual perception proceed in sync without delay. Responses should not come at the cost of missing new visual input; perception and reasoning must remain temporally aligned. Regarding the purple segment depicted in Fig. 1, maintaining synchronization is crucial to prevent missed answers. This requires answering while continuously observing, with zero latency, while also ensuring time and memory efficiency as the number of incoming frames grows over time.

Unfortunately, existing evaluation frameworks [51, 27, 26, 61, 13] and streaming models [5, 52] fall short in supporting or measuring the unified capabilities of proactive, just-in-time, and synchronized reasoning—and often struggle even with some individual aspects. Offline video benchmarks [14, 66, 30, 50, 1] evaluate video LLMs across diverse question types and scenarios, but their offline nature limits the assessment of the three core capabilities essential for online deployment. Recent efforts toward online and streaming benchmarks address this gap by introducing proactive tasks. Nevertheless, as shown in Tab 1, they often offer limited question diversity, lack contextual continuity across queries, and—more importantly—rarely evaluate just-in-time responsiveness or synchronized efficiency. As a result, current online video LLMs remain confined to narrow tasks such as narration or simple question answering, lacking the capacity for continuous, multi-turn understanding. More critically, as illustrated in Fig. 6, these models exhibit poor just-in-time behavior—often generating under-responsive or over-extended answers. Similarly, although recent efforts [51, 33] have begun to address efficiency, they tend to focus solely on accelerating response generation—potentially at the cost of answer accuracy—while overlooking the need to balance perception and answering under synchronized constraints.

As a first step toward addressing these challenges, we introduce *a new Ego STreaming Proactive (ESTP) benchmark and evaluation framework*, specifically designed to capture the demands of the three key properties in streaming video. **For proactive coherence**, all question-answering tasks in the benchmark are proactive in nature: each question can only be answered based on future video streams

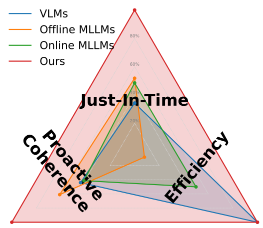

Figure 2: ESTP Triangle of Impossibility shows trade-offs among the three dimensions: Proactive Coherence, Just-in-Time responsiveness, and Efficiency, which are quantified by contextual performance, recall, and FPS.

Dataset	Ques. Type	Proactive Type			JIT Responsiveness Eval.			# Ques.
		Exp.	Imp.	Cont.	Ans. Turn	Is Prec.	Timeliness	
Online Benchmark								
VStream [61]	OE	✘	✘	✘	S	✘	✘	3,500
StreamingBench [27]	MC	✘	✘	✘	S	✘	✘	4,500
StreamingBench (PO) [27]	Q-Match	✔	✘	✘	S	✘	✔	50
OVO-Bench [26]	MC	✘	✘	✘	S	✘	✘	2,814
OVO-Bench (FAR) [26]	C & Q	✔	✘	✘	M	✔	✘	1618
MMDuet [51]	OE	✔	✘	✘	M	✘	✔	2000
Ego Benchmark								
EgoPlan [6]	OE	✘	✘	✘	S	✘	✘	5,000
EgoPlan2 [35]	OE	✘	✘	✘	S	✘	✘	1,300
EgoSDQES [13]	Q-Match	✔	✘	✘	S	✔	✔	3,971
ESTP (Ours)	OE	✔	✔	✔	M	✔	✔	2264

Table 1: Comparison of datasets based on proactive and streaming criteria. This table summarizes datasets by Question Types (Open-Ended (OE); Multiple Choice (MC); Query Matching (Q-Match & Q); and Count (C)), Proactive Types (Explicit (Exp.); Implicit (Imp.); and Contextual (Cont.)), and Just-in-Time (JIT) Responsiveness. Key JIT Responsiveness aspects include Answer Turn (Ans. Turn) (options: Single (S), Multi (M)), Precision (Is Prec.), and Timeliness. The notation '# Ques.' denotes the number of questions.

within one or more specific time intervals. To reflect different levels realistic scenarios, we group them into three types: (1) explicit, grounded in clear visual cues; (2) implicit, requiring reasoning beyond surface observations; and (3) contextual, involving temporally linked questions that demand consistent multi-turn answers. We collect 2,264 questions spanning 14 task types—such as object localization, state change understanding, and intention prediction—across over 100 types of distinct scenarios, including kitchen activities, social interactions, and daily object manipulation. **For just-in-time responsiveness**, we emphasize the importance of response timing: each question are annotated an average of 3.96 valid answer intervals, and a prediction is considered valid only if it falls within the designated window. To assess this, we introduce ESTP-F1, a metric that integrates answer quality, response timing, and temporal precision. Additionally, 46% of questions are contextually linked, requiring coherent responses based on prior questions—highlighting the need to continuously track the evolving stream from past to future and respond at the right moment. **For synchronized efficiency**, we not only evaluate time and memory efficiency and answering accuracy independently, but also assess accuracy under tightly synchronized perception and response—offering a comprehensive perspective on streaming video LLM evaluation.

To address this novel task, ***we propose a comprehensive and novel technical pipeline—including a data engine, multi-stage training strategies, and a proactive dynamic compression technique—to enhance the streaming video LLMs. Specifically***,

- **The data engine** automatically generates diverse, multi-turn questions and their corresponding answers to support the demands of continuous and proactive question answering. This involves a three-stage generation pipeline covering (1) one-to-one: using LVLMs to generate captions and extract initial question-answer pairs with a single temporal answer interval; (2) one-to-many: applying RAG to expand each answer into multiple valid intervals; and (3) many-to-many: composing coherent multi-turn questions from related QA pairs.
- **The multi-stage training strategy** is employed to progressively learn: (1) passive interval responsiveness, which provides a basic ability to trigger responses by distinguishing visually similar frames with different response labels, but often results in over-responsiveness even when the correct response interval; (2) Proactive just-in-time responsiveness and accurate answering, which trains the model to actively request high-resolution frames during uncertain timestamps, allowing it to use fine-grained visual details to pinpoint both the correct response moment and the accurate answer; (3) Coherence across multi-turn QA, which enables the model to maintain consistency by reasoning over prior QA history and current context, supporting contextual consistency answering.
- **The proactive dynamic compression** technique fully leverages the streaming nature by applying two levels of token compression based on response likelihood, including: (1) when the model anticipates a potential response, it proactively requests high-resolution inputs to improve the accuracy of perception and answering; (2) Otherwise, it applies a higher compression rate to past content to reduce token usage and improve efficiency; (3) Additionally, once a response is completed, the content preceding its timestamp is further compressed to free up resources without affecting future perception or answering.

In summary, our contributions include: the novel Ego-Streaming Proactive (ESTP) task, distinguished by its three key properties; the ESTP-Bench benchmark and the ESTP-F1 metric for robust evaluation of this task; and a comprehensive and novel technical pipeline, incorporating three key techniques, designed to address the ESTP task. Our results demonstrate that the proposed model effectively overcomes the key challenges posed by this task. Moreover, it demonstrates superior performance by substantially exceeding multiple baselines in diverse online and offline benchmarks.

2 Ego Streaming Proactivate Dataset & Benchmark

2.1 Data Source and Annotation

Data Source is validation set of Ego4D [17, 44] that includes raw annotations such as event narrations and steps for completing consistent goals. Following [28, 5], we filtered out video with missing or uncertain annotations and converted annotations into a natural language format. This process yielded 890 videos, encompassing over 100 distinct scenes and a wide array of human activities, including indoor home environments (e.g., cooking, cleaning), workspaces (e.g., working at desk, labwork, baker), and public areas (e.g., grocery shopping). Furthermore, the videos exhibit rich dynamic diversity, ranging from periods of relative stillness (e.g., observing a static scene) to highly dynamic moments involving rapid manipulation tasks or active locomotion (e.g., cooking, walking).

Annotation process follows a two-step procedure. First, initial QA pairs are automatically generated with the assistance of MLLMs [56, 49] and LLMs [10]. Second, these automatically generated questions provided inspiration for annotators, aiding them in identifying valuable instances or formulating question ideas. To ensure diversity of questions, we annotate three proactive types:

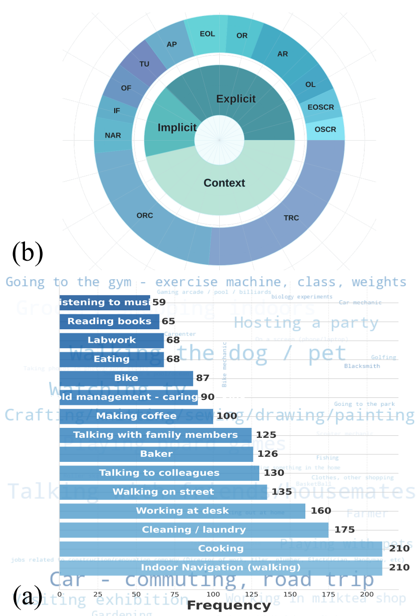

Figure 3: (a) Frequency of scenes or activities from which tasks and questions are derived. (b) Proportion of different proactive and question task types.

(1). ***Explicit Proactive Tasks*** are defined as those required to identify and respond to queries by directly leveraging and interpreting visual information present in the input. This category encompasses tasks where the relevant visual cues are explicitly referenced or are central to formulating a correct response. This category is comprised of eight distinct task types: Object Recognition (OR), Attribute Perception (AP), Text-Rich Understanding (TRU), Object Localization (OL), Object State Change (OSC), Ego Object Localization (EOL), Ego Object State Change (EOSC), and Action Recognition (AR). **(2).** ***Implicit Proactive Tasks*** are defined as those requiring inference and deeper scene understanding that goes beyond immediate, direct observation. This category is comprised of four distinct task types: Object Function Reasoning (OFR), Information Function Reasoning (IFR), Next Action Reasoning (NAR), and Task Understanding (TU). **(3).** ***Contextual Proactive Tasks*** are defined as those requiring the model to maintain awareness of dialogue history and visual coherence across temporally extended interactions. This category is comprised of two distinct task types: Object Relative Context (ORC) and Task Relative Context (TRC). Fig. 3 illustrate dataset distribution.

To enable the evaluation of Just-in-Time Responsiveness and eliminate ambiguity in answer intervals, human annotators are required to mark clear time interval boundaries based on the completeness of objects within frames or the start/end of events. Simultaneously, questions with ambiguous references are filtered out (e.g., "Remind me the location of the ceramic bowl." where multiple ceramic bowls might be present in different locations). Each sample's question, answer, and corresponding answer interval are verified by two annotators. This rigorous verification process resulted in a dataset of 2264 verified question-answer instances. Notably, every answer in the dataset is associated with precise temporal annotations. Statistical information regarding the annotated data is presented in Fig. 3.

2.2 Evaluation Metric in ESTP

To comprehensively measure performance along three key evaluation aspects – answer quality, response timing, and temporal precision – we introduce the ESTP-F1 score. Here, we denote a ground truth item as g_k with content o_k, and a prediction as $\hat{p}_l$ with content $\hat{o}_l$ and time $\hat{t}_l$. Evaluation components are defined for matched pairs $(\hat{p}_l, g_k)$, where $\hat{p}_l$ is a prediction that temporally matches g_k. For answer quality, an LLM [10] is used to measure correctness, defined as a score $\mathcal{S}_{\text{answer}}(\hat{o}_l, o_k)$ for the predicted content $\hat{o}_l$ relative to the ground truth content o_k. For evaluating response timing, we go beyond simply considering recall (which inherently accounts for False Negatives (FN)) and employ a score $\mathcal{S}_{\text{time}}(\hat{t}_l, g_k)$ to more precisely measure timeliness. Furthermore, for temporal precision, we introduce precision, utilizing False Positives (FP) as a penalty term. These components contribute to the aggregated ground truth score $S(g_k)$, which replaces the traditional binary TP count. The ESTP-F1 score is computed as:

$$\text{ESTP-F1} = \frac{2 \times \sum_{k=1}^{M} S(g_k)}{2\sum_{k=1}^{M} S(g_k) + \mathsf{FP} + \mathsf{FN}}, \tag{1}$$

where M is number of GT. High answer quality (reflected by a high S_{answer} score), effective response timeliness (characterized by high S_{time} for on-time responses and a low False Negative (FN) rate), and high precision (indicated by a low False Positive (FP) rate) collectively contribute to a high ESTP-F1 score. More details are provided in the Appendix.

3 Methodology: VideoLLM-EyeWO

In this section, we introduce a technical pipeline designed for the ESTP task. For the data engine, utilizing the Ego4D [17] training set and a three-stage generation pipeline as introduced in Sec. 1, we generate 60K single-turn and 20K multi-turn questions, as shown in Fig. 4. Each generated instance includes questions, answers, and their corresponding valid answer intervals (named as ESTP-IT). See Appendix for data engine details. Subsequently, we detail the problem definition and preliminary, the multi-stage training strategies, and the proactive dynamic compression technique in respective subsections.

3.1 Problem Definition and Preliminary

Problem Definition. Given a streaming video input and a sequence of emerging queries $\mathcal{Q} = \{(q_i, t_{q_i})\}$, where q_i is the query content and t_{q_i} is the query timestamp. At each timestep t following a query (i.e., $t > t_{q_i}$), the model must leverage its historical memory H_t (including visual input history and past query-response interactions) , while concurrent observation O_t, to decide whether to perform a response action and generate corresponding content. The model's decision-making process at time t can be formulated as selecting the optimal action A_t from a predefined set A:

$$A_t = \text{argmax}_{a \in A}\, P_\theta(A_t = a \mid q_i, O_t, H_t). \tag{2}$$

Here, θ represent model parameter, A_t is the model's action at time t, and A is the set of possible actions. Notably, while previous work typically considers an action space that only includes a_{silence} (staying silent) and a_{response} (executing a response and generating a reply), we expands this by including the action $a_{\text{ask\_high}}$ (requesting a high-resolution frame), as introduced in Sec. 3.2 Stage-1.

Preliminary. LIVE [5] utilizes ground truth containing timestamps and applies cross-entropy supervision [48] to the model's action output at each timestep. Specifically, if the current time t falls within a ground truth response region (denoted as $t \in \mathcal{T}_{\text{timestamp}}$), the model is supervised to execute the response action (a_{response}) and generate a reply, incorporating a language modeling loss $\mathcal{L}_{\text{LM}}$ [59, 11, 48]. Otherwise, it is supervised to remain silent (a_{continue}). This is formulated as:

$$\mathcal{L}(t) = \begin{cases} -\log P_\theta(a_{\text{response}} \mid q_i, O_t, H_t) + \omega\mathcal{L}_{\text{LM}}(t) & \text{if } t \in \mathcal{T}_{\text{timestamp}} \\ -\log P_\theta(a_{\text{continue}} \mid q_i, O_t, H_t) & \text{otherwise,} \end{cases}, \tag{3}$$

where, ω is a balancing coefficient weighting the language modeling objective.

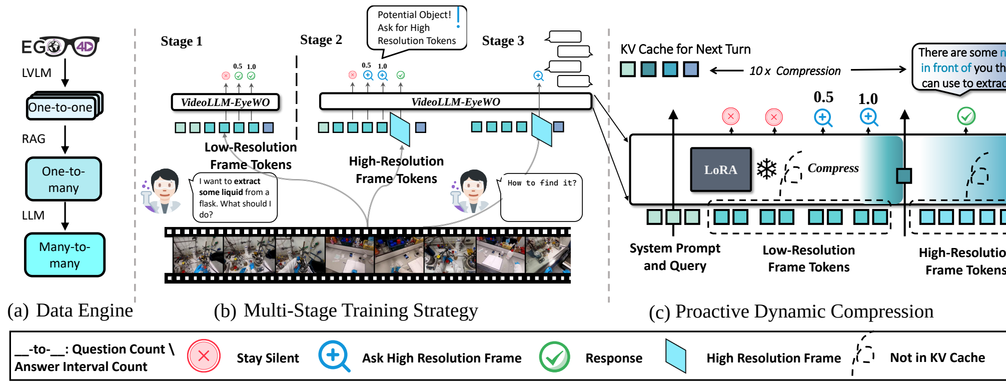

Figure 4: Overview of the proposed pipeline. The figure illustrates the three main components: (a) **Data Engine** (ESTP-Gen), which automatically generates diverse, multi-turn QA data through a three-stage pipeline. (b) **Multi-Stage Training Strategy** incrementally builds the model from basic responsiveness to proactive just-in-time accuracy, and ultimately to achieving multi-turn coherence, detailed in Section 3.2. (c) **Proactive Dynamic Compression** detailed in Section 3.3.

3.2 Multi-Stage Training Strategy

Following [5], VideoLLM-EyeWO utilizes the same network architecture and is trained using LoRA [20]. However, the single-stage training and simple binary supervision strategy employed in [5] can lead to training conflict due to the high similarity of adjacent frames in streaming inputs. This conflict necessitates a difficult trade-off between over-extended and under-responsive. To address these limitations, we employ a multi-stage training strategy designed to progressively endow the model with response capabilities. The following subsections detail each stage of this training strategy.

Stage-1 : Passive Interval Responsivenes. To provide the basic ability for autonomous response triggering, we leverage the valid answer intervals within the ESTP-IT to achieve a progressive transition from silence to response. Specifically, if current time t falling within a valid answer interval (where $\mathcal{T}_{\text{interval}}$ is defined as the set of all such intervals $[s_i, e_i]$), we apply a weighted degree of response supervision, rather than direct binary classification, using the following loss function:

$$\mathcal{L}(t) = \begin{cases} -\log\left(f\left(\frac{|t-e\,|}{|s-e\,|}\right) \cdot P_\theta(a_{\text{response}} \mid q_i, O_t, H_t) \right) + \omega \mathcal{L}_{\text{LM}}(t) & \text{if } \exists [s,e] \in \mathcal{T}_{\text{interval}}, t \in [s,e] \\ -\log P_\theta(a_{\text{continue}} \mid q_i, O_t, H_t) & \text{otherwise} \end{cases}, \tag{4}$$

The function f is a linear decrease map used as a weighting factor applied to the response probability loss. The highlight in Equ. 4 is used to distinguish the components specific to this stage.

Stage-2 : Proactive just-in-time responsiveness and accurate answering. To use fine-grained visual details to pinpoint both the correct response moment and the accurate answer, we train the model to actively request high-resolution frames during uncertain timestamps in this stage. Specifically, we first introduce a third predefined action $a_{\text{ask\_high}}$. When the model executes this action at time t, it triggers the acquisition of the high-resolution frame O_t^h corresponding to the current observation O_t using the following loss function for training: $\mathcal{L}_{\text{ask\_high}}(t)$:

$$\mathcal{L}_{\text{ask\_high}}(t) = \begin{cases} -\log\left(f\left(\frac{|t-e|}{|s-e\,|}\right) \cdot P_\theta(a_{\text{ask\_high}} \mid q_i, O_t, H_t) \right) & \text{if } t \in \mathcal{T}_{\text{uncertain}} \\ -\log P_\theta(a_{\text{continue}} \mid q_i, O_t, H_t) & \text{otherwise,} \end{cases}, \tag{5}$$

where $\mathcal{T}_{\text{uncertain}}$ denotes the set of the model's uncertain (see more detail in Appendix D Stage-2 Input). We use this loss to enable the model to acquire the ability to request high-resolution frames, and then based on the more detailed information, determine whether it is the correct time to respond and provide a more accurate answer, using the following loss:

$$\mathcal{L}_{\text{determine}}(t) = \begin{cases} -\log\ P_\theta(a_{\text{response}} \mid q_i, O_t, H_t,\ O_t^h\ ) + \omega \mathcal{L}_{\text{LM}}(t) & \text{if } t \in \mathcal{T}_{\text{timestamp}} \\ -\log P_\theta(a_{\text{continue}} \mid q_i, O_t, H_t,\ O_t^h\ ) & \text{otherwise} \end{cases}, \tag{6}$$

where O_t^h represents the high-resolution frame acquired at time t. The overall loss function at timestep t is the sum of the two components:

$$\mathcal{L}(t) = \mathcal{L}_{\text{ask\_high}}(t) + \mathcal{L}_{\text{determine}}(t) \tag{7}$$

See appendix for detailed uncertain timestamps $\mathcal{T}_{\text{uncertain}}$ identified.

Stage-3 : Coherence across multi-turn QA. Building upon the model's acquired proactive and timely response capabilities, we introduce a separate training stage. Specifically, this stage involves training solely on multi-turn question, with the aim of further improving its contextual understanding while preserving its timely responsiveness.

3.3 Proactive Dynamic Compression Mechanism

In order to ensure memory efficiency as the number of incoming frames grows over time, we propose the Proactive Dynamic Compression Mechanism, which applies two levels of token compression and employs a uniform compression method, detailed respectively in the following two subsections.

Two-Level Compression. In contrast to fixed compression rates [29, 34, 4] and steps [43, 39, 58, 63], our mechanism leverages the streaming nature to allow the model to proactively determine both when to compress and which compression level to apply. Regarding the timing of compression, after the model generates a response, the preceding visual input and the response content itself form a natural segment or processing unit. Simultaneously, lower compression rates are applied to question-relevant content such as high-resolution frames, while higher rates are applied to other content, with these decisions proactively made by the model. Specifically, after a response, a fixed number of compression tokens (e.g., 1) are used to compress the preceding content, absorbing information from potentially many low-resolution frames or a single high-resolution frame. This approach naturally achieves a high compression rate for redundant parts of the past content, resulting in an average token usage of only about one-tenth of the original sequence.

Uniform Compression Method. For achieving two-level compression, we employ a Uniform Compression Method. Specifically, unlike methods using additional compression modules [34, 33], we insert a special compression token ($\langle \text{ct} \rangle$) after segments of original input, namely after single high-resolution frames, after multiple low-resolution frames, and after answer. This token is initialized using the text embedding of the "<EOS>" token. Leveraging the properties of the causal self-attention mechanism, this token prompts the LLM to compress the information from the preceding segment into a compact representation stored in the KV cache.

During training, inspired by [43], the LLM is trained to process response turns sequentially. A response turn refers to a turn of interaction, typically a comprising visual input and a model's response. Training for the Proactive Dynamic Compression Mechanism, including the integration of high-resolution frame requests, commences in Stage 2 of our multi-stage training strategy to ensure manageable training memory overhead.

4 Experiment

4.1 Baseline and Evaluation Settings

We evaluate three categories of models in this study: Offline MLLMs, VLMs, and Online MLLMs.

For **Offline MLLMs** we selected representative models from different open-source MLLM families, including LLaVA-OneVision [23], Qwen2-VL [49], MiniCPM-V [56], LLaVA-NeXT-Video [24], and InternVL-V2 [7]. As offline MLLMs lack inherent proactive response capability, following previous studies [27, 26, 51, 5], we employed two evaluation settings: (1) *Response-in-Last*: The model processes the complete video and is tasked with generating textual reply with timestamps. (2) *Polling Strategy*: The model is periodically queried at fixed time intervals. If the model indicates readiness, it is then prompted to generate the answer. Specific details regarding the prompts and hyperparameter used in these settings are provided in Appendix.

Regarding **VLMs**, following the approach of SDQES [13], we selected CLIP [36], LaViLa [64], and EgoVLP [28] for evaluation. These models were evaluated by computing the similarity between each frame and the query, using 0.5 as the threshold to determine responsiveness. Notably, as these models cannot generate open-ended replies, their reply score is set to 0.

Model	Explicit Proactive Task									Implicit Proactive Task					Contextual Q			Overall
	OR	AP	TRU	OL	OSC	EOL	EOSC	AR	All	OFR	IFR	NAR	TU	All	ORC	TRC	All	
Offline MLLMs Response-in-Last																		
LLaVA-OneVision	7.2	11.5	4.9	10.0	4.9	6.9	5.6	3.2	6.8	3.8	6.3	11.6	29.8	12.9	10.8	5.7	8.2	8.7
Qwen2-VL	11.7	8.1	14.9	10.5	1.7	8.9	10.6	6.0	9.0	10.2	4.4	26.5	49.5	22.6	13.3	9.4	11.3	13.3
MiniCPM-V	12.3	12.6	10.7	13.7	8.6	7.5	11.9	5.5	10.4	11.8	9.2	36.0	55.3	28.1	32.6	25.4	29.0	18.1
LLaVA-NeXT-Video	8.3	9.4	7.4	10.2	7.8	7.4	10.3	5.6	8.3	6.4	6.7	21.1	45.9	20.0	10.1	9.8	9.9	11.9
InternVL-V2	9.3	14.6	9.5	10.6	1.7	6.3	3.0	3.6	7.3	3.3	9.2	15.5	28.2	14.0	16.9	15.6	16.2	10.5
VLMs for Streaming Detection																		
CLIP	7.3	9.5	7.4	8.5	1.8	4.7	2.2	2.7	5.5	2.8	5.2	51.3	29.3	22.2	4.6	3.8	4.2	10.1
LaViLa	8.4	10.7	9.0	9.1	3.1	5.4	3.6	4.3	6.7	7.8	10.0	56.2	34.4	27.1	9.4	28.9	19.2	14.3
EgoVLP	10.5	11.0	8.7	8.5	5.5	5.6	5.3	4.4	7.4	6.2	10.7	58.4	48.3	30.9	8.0	25.3	16.6	15.5
Offline MLLMs Polling Strategy																		
LLaVA-OneVision	8.3	8.8	22.8	25.4	13.5	9.8	9.6	10.3	13.6	20.3	20.9	35.9	49.9	31.8	14.6	1.9	8.2	18.0
Qwen2-VL	13.7	13.5	15.4	29.5	8.0	15.4	16.6	10.9	15.4	17.8	19.8	56.4	63.1	39.3	13.0	7.7	10.4	21.3
MiniCPM-V	14.9	16.8	17.1	26.8	7.7	12.9	12.5	13.1	15.2	15.9	21.0	46.8	62.2	36.5	24.3	28.9	26.6	22.9
LLaVA-NeXT-Video	15.6	14.6	21.9	26.8	12.8	14.2	13.5	12.3	16.5	18.6	23.2	44.9	51.6	34.6	19.9	7.7	13.8	21.3
InternVL-V2	11.3	5.9	7.0	10.1	0.7	2.7	5.2	2.2	5.6	8.3	2.9	4.3	11.2	6.7	6.1	5.3	5.7	5.9
Online MLLMs																		
LIVE(threshold=0.8)	9.7	11.0	7.4	10.8	1.9	6.0	3.6	5.6	7.0	4.2	7.4	12.9	12.8	9.3	19.6	13.8	11.8	9.1
LIVE(threshold=0.9)	11.2	13.9	7.9	13.2	5.6	9.4	6.0	8.9	9.5	5.8	8.9	41.0	46.7	25.6	11.3	26.5	18.9	15.5
MMDuet	7.2	10.3	17.6	10.2	4.2	6.1	8.8	8.5	9.1	10.0	7.7	50.1	69.1	34.2	17.4	23.1	20.3	17.8
VideoLLM-EyeWO(Ours)	**26.6**	**26.6**	**25.1**	**26.8**	**19.8**	**22.3**	**20.8**	**20.7**	**23.6**	**24.8**	**31.0**	**75.3**	**78.7**	**52.5**	**39.5**	**47.8**	**43.6**	**34.7**

Table 2: Experimental results of various models evaluated on the ESTP-Bench. We present performance across Explicit Proactive, Implicit Proactive, and Contextual Question task types, as well as the Overall score, for Offline MLLMs (Response-in-Last and Polling Strategy), VLMs for streaming detection, and Online MLLMs. Deep blue highlights the best overall performance, while blue indicates the best performance within each model category and evaluation setting group.

For **Online MLLMs**, we selected VideoLLM-Online [5] and MMDuet [51], which provide open-source weights and streaming inference code, for evaluation. For VideoLLM-Online, we experimented with different thresholds to assess its performance variations.

4.2 Benchmarking in ESTP-Bench

Comparative Analysis of Baseline Models. Tab. 2 shows the performance of different models across three proactive types and fourteen task types under various evaluation settings, the experimental results consistently demonstrate that ESTP tasks pose significant challenges for all current types of models. Analysis revealed variations across model categories, with certain models exhibiting stronger capabilities within their respective groups (e.g., MiniCPM-V [56] and QwenVL-2 [49] among offline MLLMs aligning with previous work [8], and temporal VLMs like LaViLa [64] and EgoVLP [28] outperforming spatially-focused models like CLIP [36]). Furthermore, the evaluation strategy significantly impacts performance. Specifically, offline MLLMs showed a notable disparity, performing on average better under the Polling Strategy compared to the Response-in-Last strategy, with improvements up to 5.4%. This highlights the effectiveness of ESTP-Bench in evaluating models from a timeliness perspective and underscores the limitations in temporal grounding of existing offline models.

Performance of VideoLLM-EyeWO Against Baselines. As presented in Tab. 2, our proposed model achieved significant performance improvements across all proactive tasks. Compared to the baseline videoLLM-Online [5], our model demonstrated an improvement of +19.2%. Furthermore, it outperformed the best-performing model, MiniCPM-V [56](using the Polling strategy), by +11.8%.

4.3 In-Depth Analyses in ESTP-Bench

Challenges with Coherent and Contextual Questions: Fig. 5 illustrates the average performance of different models across 14 tasks. (NAR) and (TU) exhibit significantly higher performance compared to other tasks. Upon visualizing the proportion of valid answer intervals relative to the input video duration for these two tasks, we observe that this proportion is substantially higher than for other tasks. This is attributed to these annotations originating from the raw GoalStep [44] labels, which involve segmenting continuous actions towards a consistent goal, thereby leading to a larger proportion of valid answer interval within the video and consequently, higher Recall. Conversely, for the (TRC) task, which also derives from the same original annotations and possesses a high proportion of valid answer interval, both Recall and overall performance significantly decrease. This marked performance drop underscores the significant challenge that proactive coherence and understanding contextual information pose for existing models.

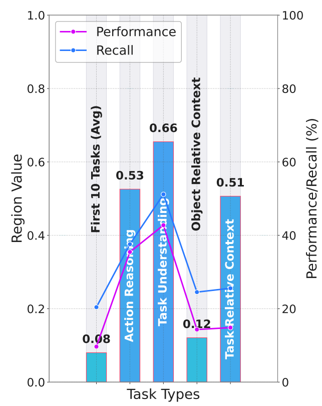

Figure 5: Average performance and Ground Truth interval proportion across 14 tasks, illustrating challenges with coherent and contextual questions.

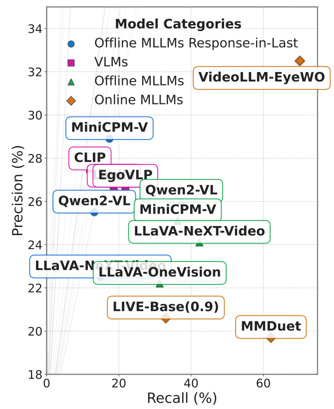

Figure 6: Recall-Precision tradeoff for different models and evaluation settings, highlighting the difficulty in responding only when necessary.

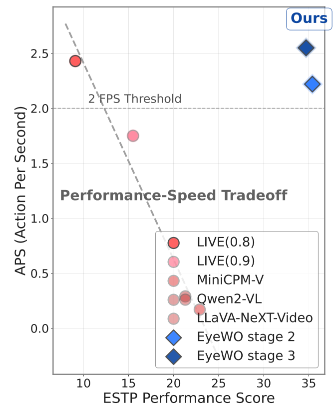

Figure 7: Action Per Second versus ESTP Score for various models, measured on an A40 GPU, demonstrating synchronization efficiency challenges.

Difficulty in Responding Only When Necessary: Fig. 6 presents the relationship between recall and precision for different models under various evaluation settings. We observe a prevalent negative correlation between recall and precision among most models. For instance, MMDuet achieves exceptionally high recall but at the expense of low precision. This trade-off indicates the struggle of existing models to provide proactive yet precise responses.

Synchronization Efficiency Challenges: Fig. 7 illustrates the inherent performance-speed tradeoff in ESTP tasks by plotting Action Per Second (APS) against Performance Score for various models. Existing methods often lie along a clear tradeoff curve, where higher performance is typically associated with lower APS, highlighting the difficulty in achieving both simultaneously. As seen for offline MLLMs using the Polling strategy, achieving high performance while maintaining sufficient speed for real-time synchronization remains challenging. Even approaches near the input frame rate (e.g., LIVE at $\sim$2 FPS) may demonstrate suboptimal performance. This underscores the significant challenges current models face in achieving both high task performance and effective synchronization with the dynamic video stream.

4.4 Evalutation of VideoLLM-EyeWO

Evaluating Zero-Shot Capability in Online/Offline Tasks. Table 3 presents a performance comparison of our model against the baseline on both online and offline tasks. We selected VideoLLM-online [5] as our baseline, given that it shares the same base model (LLaMA3 [16] and SigLIP [60]) and data source (Ego4D) as our own mode. For the online task, we utilize OvO-Bench [26] as a recognized benchmark. For the offline task, following [12], we evaluate our model on the multiple-choice subset of the QAEGO4D-test benchmark [3]. The 'Online' setting involves posing questions as soon as the relevant answer segment appears, whereas the 'Offline' setting involves questioning after the entire video has been presented. The experimental results demonstrate the generalization capability of our model across these distinct tasks.

Model	Online Task: OVO-Bench											Offline Task	
	Real-Time Perception							Backward Tracing				QAEGO4D$_{MC}$	
	OCR	ACR	ATR	STU	FPD	OJR	**Avg.**	EPM	ASI	HLD	**Avg.**	Online	Offline
VideoLLM-online	8.05	23.85	12.07	14.04	**45.54**	21.20	20.79	22.22	18.80	**12.18**	17.73	29.80	30.20
Ours (VideoLLM-EyeWO)	**24.16**	**27.52**	**31.89**	**32.58**	44.55	**35.87**	**32.76**	**39.06**	**38.51**	6.45	**28.00**	**36.20**	**33.00**

Table 3: Detailed Performance Evaluation on OVO-Bench [26] and QAEGO4D [3] Tasks.

Evaluating Architecture Generalizability on Offline Tasks As presented in Tab. 4, our model demonstrated comprehensive performance improvements on five tasks related to traditional temporal summarization and forecasting problems. The performance gain reached up to +2.8%, which indicates that our proposed model architecture can effectively generalize to other offline tasks.

Method	COIN Benchmark				
	Step	Task	Next	Proc	Proc+
ClipBERT [22]	30.8	65.4	-	-	-
VideoLLM-online-7B-v1 [5]	59.8	92.1	44.7	47.9	52.9
VideoLLM-online-8B-v1+ [5]	63.1	92.6	49.0	49.7	53.6
VideoLLM-MOD [52]	63.4	92.7	49.8	49.8	53.3
Ours (LLaMa3 [16, 47])	<u>65.9</u>	<u>92.7</u>	<u>50.9</u>	<u>50.8</u>	<u>54.7</u>
Ours (LLaMa3.1 [16, 47])	**66.0**	**93.3**	**51.5**	**51.1**	**55.5**

Table 4: COIN [46] Benchmark Top-1 Accuracy comparison across different methods.

4.5 Ablation Study of VideoLLM-EyeWO

Method	Single Question		Contextual Question	
	Performance ↑	KV Cache Size ↓	Performance ↑	KV Cache Size ↓
LIVE	14.9	9636.0	18.9	31199.5
+ ESTP-IT	22.0	7859.1	25.7	28236.4
Stage-0	24.9	7988.2	23.0	17567.6
with increased proactive dynamic compression mechanism				
+ Stage-1 ask high frame	**34.0**	1182.8	38.7	3731.8
+ Stage-2	33.2	942.0	**43.6**	3242.8

Table 5: Ablation study results on ESTP bench

Tab. 5 details the results of our ablation study on the ESTP benchmark:

1. (+*ESTP-IT*) enhanced the LIVE baseline's performance on both Single and Contextual Question tasks, increasing it by +7.1 and +6.8 respectively, **thereby demonstrating the effectiveness of ESTP-IT**.
2. (*Stage-0*) addressed the training conflicts stemming from simple binary supervision, enabling performance improvements without requiring any manual threshold tuning, **which demonstrates the model's acquisition of a basic ability to trigger responses**.
3. With the increased proactive dynamic compression mechanism, the model's KV cache consumption was significantly reduced, **requiring on average only about 0.11% of the baseline**.
4. (+*Stage-1*) significantly boosted Single Question performance to 34.0 and Contextual Question performance jumped to 38.7 by **incorporating the mechanism for actively requesting high-resolution frames for scrutiny alongside initial compression**.
5. (+*Stage-2*) **further improved contextual coherence and refined compression**, enabling the model to achieve a gain of +4.9 on Contextual tasks, reaching 43.6. Simultaneously, the more accurate and efficient responses further reduced memory consumption to minimal levels.

5 Conclusion

We definite an novel AI assistant's task of proactive, synchronized question answering from ego-streaming video, targeting the key properties of proactive coherence, just-in-time responsiveness, and synchronized efficiency. Our contributions—the ESTP-Bench with its ESTP-F1 metric for evaluation, and a novel technical pipeline incorporating a data engine, multi-stage training, and proactive dynamic compression—enable our model to effectively tackle these properties. This approach outperforms multiple baselines across diverse online and offline benchmarks.

Acknowledgement: This work is supported in part by the National Natural Science Foundation of China under Grant No.62206174 and No.62576365.

In the Appendix, we provide additional information regarding,

- Related Work in Sec. A
- ESTP-Bench: Dataset and Evaluation Details in Sec. B
- Model Input Example in Sec. C
- Training Implementation Detail in Sec. D
- ESTP-Bench Evaluation Details in Sec. E
- Limitation and Future Work in Sec. F
- Data Examples in Sec. G
- Qualitative Results in Sec. H

A Related Work

Streaming Video Understanding. Unlike traditional offline video understanding tasks [14, 66, 1, 50] which only allow for question answering after processing the entire video, Online Video Understanding tasks aim to evaluate the ability to respond to questions that arise at any time, based on past information and current observations from a sequential video stream input. Previous work [61, 26, 27] has employed various question types presented during the video stream, such as object or event perception, leveraging different spatiotemporal cues to comprehensively evaluate streaming video understanding capabilities. However, for proactive tasks where questions often require reasoning [65] beyond the current frame, existing methods often exhibit limited question diversity and lack contextual continuity across queries. Furthermore, evaluation in previous work has often overlooked efficiency and timeliness.

To specifically endow MLLMs [42] with proactive response capability, VideoLLM-Online [5] proposed the LIVE training framework, which supervises the model's output at each frame. Subsequent work has focused on improving training efficiency [52], inference speed [33], and response capability [51]. However, these methods often generate under-responsive or over-extended answers and struggle to adapt to continuous, multi-turn conversation.

Egocentric Video Understanding. Compared to traditional third-person video understanding, egocentric video data poses unique challenges, such as the scarcity of large-scale annotated datasets and the inherent narrow and often unstable viewpoint. However, recent work [17, 18, 9, 44] has contributed massive egocentric video datasets and fundamental annotations, significantly benefiting the community. Prior work has typically focused on classic egocentric video understanding tasks such as activity recognition [25, 38], temporal grounding [55, 31, 41], and hand-object detection [2, 21], which are often limited by a closed vocabulary. Other efforts have focused on offline video understanding tasks, such as QaEgo4D [3], EgoSchema [30], and MM-Ego [57]. While SDQES [13] introduced a streaming detection benchmark for egocentric video, it primarily evaluates similarity-based responsiveness and lacks the scope to assess the open-ended generative and conversational capabilities required from Online MLLMs in proactive scenarios.

B ESTP-Bench: Dataset and Evaluation

In this section, we first introduce the detailed description for each task within ESTP-Bench. Subsequently, we present the annotation tool and pipeline employed for these tasks. Finally, we provide a detailed description of the ESTP-F1 metric.

B.1 Task Explanation

Explicit Proactive Tasks require detecting and responding to queries that directly reference visual cues. This category includes eight distinct task types:

1. [OR] **Object Recognition**: Detect and identify specific objects.
2. [AP] **Attribute Perception**: Recognize object attributes.
3. [TRU] **Text-Rich Understanding**: Interpret and explain text content.

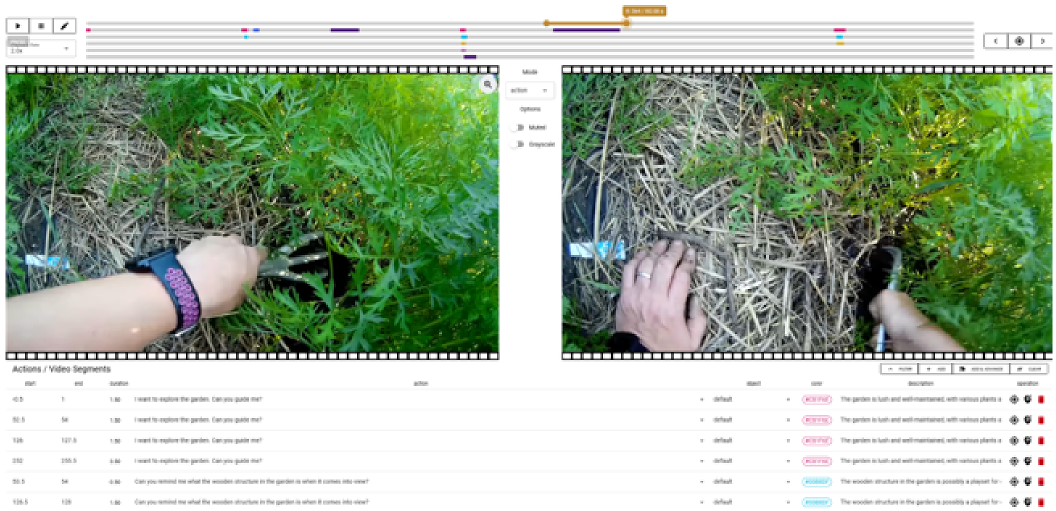

Figure 8: **Interface of the annotation tool.** This tool enables annotators to define valid answer intervals on the video timeline, author questions, and input corresponding answers. For clarity, multiple answers and their associated intervals for a single question are visually linked by a shared color.

4. [OL] **Object Localization**: Identify spatial relations between objects.
5. [OSC] **Object State Change**: Detect object state transitions.
6. [EOL] **Ego Object Localization**: Localize objects relative to the ego.
7. [EOSC] **Ego Object State Change**: Track object state changes from the ego's view.
8. [AR] **Action Recognition**: Detect and classify specific actions.

Implicit Proactive Tasks require performing inference and scene understanding beyond direct observation. Task types include:

1. [OFR] **Object Function Reasoning**: Identify functional objects and guide their use.
2. [IFR] **Information Function Reasoning**: Extract and provide information from source objects.
3. [NAR] **Next Action Reasoning**: Predict and recommend next user actions.
4. [TU] **Task Understanding**: Comprehend user goals and offer task guidance.

Contextual Proactive Tasks require maintaining dialogue history and visual coherence over time. Task types include:

1. [ORC] **Object Relative Context**: Track an object's attributes, position changes, and function across question sequences.
2. [TRC] **Task Relative Context**: Monitor user task progress, action correctness, and provide sequential guidance.

See Sec. G for data examples.

B.2 Annotation Tool and Pipeline

Annotation Tool. As shown in Fig. 8, our annotation tool [62] facilitates the labeling process: annotators can adjust the start and end timestamps of valid answer intervals in the upper region, while authoring questions in the bottom-left area and completing answers in the corresponding region on the right. Notably, a single question can be associated with multiple answers and their corresponding intervals, which are visually linked through a shared color for clarity.

Annotation Construction Pipeline. As a first step, we leverage LLMs [10] to convert raw annotations into initial question-answer pairs. For Action Recognition (AR) tasks, we utilize Ego4D [17] basic Narration raw annotations, which comprise descriptions of action-related events and their corresponding timestamps. For Next Action Reasoning (NAR), Task Understanding (TU), and Task

Relative Context (TRC) questions, we leverage Ego4D GoalStep [44] annotations, which provide a task goal, multiple task steps, and their corresponding temporal intervals. For these aforementioned tasks, we directly prompt LLMs for question generation. For all other task types, question generation is performed through the data engine.

Subsequently, the data undergoes a human annotation phase. For Action Recognition (AR), Next Action Reasoning (NAR), Task Understanding (TU), and Task Relative Context (TRC) tasks, given their origin from existing dataset [44], annotators primarily focus on three aspects: (1) detecting question ambiguity; (2) assessing the question-answer pair's matching quality and correcting erroneous wording; and (3) calibrating the answer interval timestamps. For all other task types, annotators are additionally required to generate questions and complete answers, inspired by the initial QA pairs, before executing the aforementioned refinement steps. Simultaneously, a double-check mechanism is implemented, where a second annotator independently re-executes the aforementioned three steps for verification.

B.3 Evaluation Metric (ESTP-F1)

Let $\mathcal{G} = \{g_k = (o_k, [t_k^{\text{start}}, t_k^{\text{end}}], t_k^{\text{opt}})\}_{k=1}^{M}$ denote a set of M ground truth items, where o_k is the content, $[t_k^{\text{start}}, t_k^{\text{end}}]$ is the temporal interval, and $t_k^{\text{opt}} \in [t_k^{\text{start}}, t_k^{\text{end}}]$ is the optimal response timestamp. Let $\mathcal{P} = \{\hat{p}_l = (\hat{o}_l, \hat{t}_l)\}_{l=1}^{N}$ represent the set of N predictions, where each prediction $\hat{p}_l$ consists of the predicted content $\hat{o}_l$ and a prediction timestamp $\hat{t}_l$. Following [13], we also introduce temporal tolerances: τ_{ant} (set to 1 second) for allowed anticipation before t_k^{start}, and τ_{lat} (set to 2 seconds) for allowed latency after t_k^{end}.

A prediction $\hat{p}_l$ is considered a **valid match** for a ground truth g_k if its timestamp $\hat{t}_l$ falls within the interval $[t_k^{\text{start}} - \tau_{\text{ant}}, t_k^{\text{end}} + \tau_{\text{lat}}]$. We define $\mathcal{P}_k = \{\hat{p}_l \in \mathcal{P} \mid \hat{p}_l \text{ is a valid match for } g_k\}$ as the set of all such valid matching predictions for g_k.

For each prediction $\hat{p}_l$ that is a valid match for g_k, we compute a **match quality score** $\mathcal{S}(\hat{p}_l, g_k) \in [0, 1]$ to comprehensively evaluate its quality. This score is the average of a answer accuracy score and a timeliness score:

$$\mathcal{S}(\hat{p}_l, g_k) = \frac{\text{Score}_{\text{answer}}(\hat{o}_l, o_k) + \text{Score}_{\text{time}}(\hat{t}_l, g_k)}{10}. \tag{8}$$

The $\text{Score}_{\text{answer}}(\hat{o}_l, o_k) \in [1, 5]$ evaluates the semantic correctness of the predicted content $\hat{o}_l$ against the ground truth content o_k, typically assessed by a advanced Large Language Model [10].

The $\text{Score}_{\text{time}}(\hat{t}_l, g_k) \in [0, 5]$ assesses the temporal accuracy of the prediction timestamp $\hat{t}_l$ relative to the optimal response timestamp t_k^{opt}. The definition of t_k^{opt} varies by task type:

- For tasks emphasizing immediate perception upon appearance (e.g., Object Recognition (OR), Attribute Perception (AP), Text-Rich Understanding (TRU), Object Localization (OL), Object Function Reasoning (OFR), Information Function Reasoning (IFR), and Object Relative Context (ORC)), t_k^{opt} is set to t_k^{start}.
- For all other task types that may require more observation of event progression, t_k^{opt} is the midpoint of the interval $[t_k^{\text{start}}, t_k^{\text{end}}]$, allowing sufficient time for information processing before a response.

The timeliness score is then calculated as:

$$\text{Score}_{\text{time}}(\hat{t}_l, g_k) = 5 - 5 \times \min\left(1, \frac{|\hat{t}_l - t_k^{\text{opt}}|}{\text{scale}_k}\right), \tag{9}$$

where $\text{scale}_k = \max(1, (t_k^{\text{end}} - t_k^{\text{start}}) + \tau_{\text{ant}} + \tau_{\text{lat}})$ is a normalization factor representing the total effective time window. This factor is used to prevent division by zero for point intervals (where $t_k^{\text{start}} = t_k^{\text{end}}$).

For each ground truth item g_k, an aggregated score $S(g_k) \in [0, 1]$ is determined by averaging the quality scores of its matching predictions:

$$S(g_k) = \begin{cases} \frac{1}{|\mathcal{P}_k|} \sum_{\hat{p}_l \in \mathcal{P}_k} \mathcal{S}(\hat{p}_l, g_k) & \text{if } \mathcal{P}_k \neq \emptyset \\ 0 & \text{if } \mathcal{P}_k = \emptyset \end{cases}. \tag{10}$$

This $S(g_k)$ provides a nuanced measure of performance for each ground truth item.

Finally, the **ESTP-F1 score** is calculated as:

$$\text{ESTP-F1} = \frac{2\sum_{k=1}^{M} S(g_k)}{N + M - 2\sum_{k=1}^{M} \mathbb{I}(S(g_k) \neq 0) + 2\sum_{k=1}^{M} S(g_k)} \tag{11}$$

where $\mathbb{I}(\cdot)$ is the indicator function. This metric offers a comprehensive evaluation of a model's just-in-time proactive capability by jointly considering content accuracy and temporal alignment through the $S(g_k)$ scores. **In contrast to classic detection tasks, which may generate redundant proposals for the same region, streaming proactive tasks necessitate a single, well-considered judgment at each timestamp. Therefore, rather than selecting the best among multiple redundant proposals as a True Positive (TP), our evaluation metric calculates the average of all valid matches. This approach comprehensively assesses each of the model's actions, reflecting the unique temporal nature of streaming environments.**

B.4 Data Cleaning and Filtering

To ensure the high quality and suitability of the egocentric video data for the ESTP tasks, a comprehensive data cleaning and filtering pipeline is applied, involving the following key steps:

1. Initial quality control was performed in accordance with [28] to identify and remove corrupted, incomplete, or visually ambiguous segments, ensuring the foundational integrity of the data.
2. Segments with a duration shorter than **250 seconds** were filtered out to ensure sufficient temporal context for learning proactive behaviors.
3. Segments where the narration annotation coverage fell below a threshold of **0.8** were discarded to ensure robust linguistic supervision and data richness.

This multi-stage filtering process results in a refined dataset optimized for the challenges of streaming proactive perception, ensuring both visual and linguistic fidelity.

B.5 Data Engine: ESTP-Gen

As shown in Fig. 9, for automatically generates diverse, multi-turn data, we propose **ESTP-Gen**, a data engine that leverages VLMs [56, 49] and LLMs [10] to generate diverse proactive QA data from large-scale ego video datasets like Ego4D [17]. We apply a multi-stage pipeline including *Caption Generation*, *Key Segment Extraction*, and *Multi-Level QA Generation*. For simplification, in the main paper, we consolidate the Caption Generation and Key Segment Extraction steps into the one-to-one stage. **For videos spanning several minutes, directly generating QA for all segments proves challenging for entities that are persistently visible and static, as defining clear response boundaries for such entities is often ambiguous. Instead, we solely generate relevant QA from extracted key segments and complete answers by leveraging all available captions. This approach simultaneously ensures clear response boundaries and answer completeness.** The specific details of each stage below:

Multi-Perspective Caption Generation:

- **Narration:** Origin narration [44, 17] provides basic descriptions of human actions and their corresponding timestamps, serving as a foundational reference for our caption generation process.
- **Event Caption:** The original narration is typically structured as a simple subject-verb-object phrase, merely including basic category information for the actor, action, and manipulated object. It often lacks detailed information regarding object attributes, spatial-temporal location, state, or actions beyond the basic level. To generate more detailed captions specifically for events, we first follow the video clipping approach of EgoVLP [28] to obtain event-relevant video clips based on the origin narration timestamps. Then, using lexical analysis [19], we extract the actions and interacted objects. Subsequently, we use an MLLM [56] to provide detailed descriptions of the action and the interacted object.
- **Scene Caption:** The Event Captions primarily focus on foreground directly involved in human interaction, potentially overlooking the broader background content within ego videos. Therefore, a detailed description of the video's background information is necessary to complement the Event

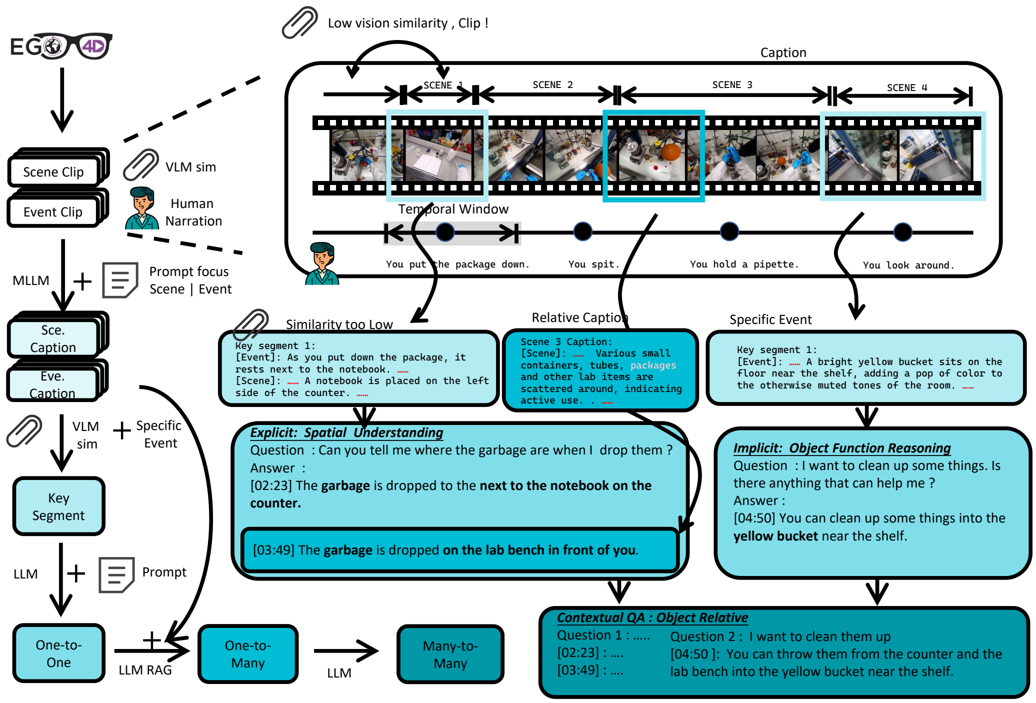

Figure 9: **ESTP-Gen Data Engine** is a multi-stage pipeline for automatically generating diverse, high-quality egocentric proactive QA data, which includes: (a) Multi-Perspective Caption Generation, creating Narration, Event, and Scene Captions to provide comprehensive foreground and background context. (b) Key Segment Extraction, identifying key segments characterized by significant visual changes and specific events. (c) **QA Generation Pipeline**, proceeding through three stages: One-to-One QA for initial pairs, One-to-Many Expansion, and Many-to-Many.

Captions. First, we perform video scene segmentation. Then, for each video segment, we prompt an MLLM [56] to generate detailed descriptions of the background context. Specifically, we utilize SigLIP [60] to extract features from each video frame and compute the change from the previous frame using cosine similarity. Potential video scene boundaries are identified where the similarity is significantly below the video's average similarity. This segmentation method, based on visual content changes, preserves the comprehensive scene content within ego videos, facilitating effective description by the MLLM.

Key Segment Extraction: Avoiding questions about persistently visible visual and static content is a key challenge for data generation of proactive task. We address this by employing two criteria for key segment extraction aimed at identifying moments suitable for generating proactive QA: specific egocentric actions and visual similarity change. The key insight is that moments in ego videos characterized by significant visual changes and scene transitions are necessarily accompanied by specific egocentric events of the actor (e.g., "turn around," "walk," "step into"). In conjunction with visual similarity analysis, we extract visual segments exhibiting viewpoint changes to serve as the basis for QA generation. As illustrated in the portion of Fig. 9, we extract key segments for QA generation. These segments are identified by significant visual changes (e.g., "scene 1") and specific event (e.g., "You look around")

- **One-to-One QA:** Using diverse prompting strategies, we guide LLMs to generate questions, visual cues, and answers from captions. As illustrated in the portion of Fig. 9, the caption of discarding a package prompted the LLM [10] to generate a question concerning the "location of dropped garbage", while the yellow bucket prompted the LLM [10] to generate a question regarding the "function of the item for helping clean".
- **One-to-Many Expansion:** We refine timestamps by aligning QA pairs with captions that fully contain the visual cues needed to answer, improving temporal coverage and QA consistency. As shown in the portion of Fig. 9, utilizing the LLM's Retrieval-Augmented Generation (RAG)

capabilities, segments with similar visual cues are identified from all remaining captions to complete all related answers.

- **Many-to-Many Contextual QA:** Logically grouped questions from the same video are combined via LLMs to form coherent multi-turn contextual QA sets. As illustrated in the portion of the Fig. 9, the questions "location of dropped garbage" and "function of the item for helping clean" exhibit logical relevance, and are therefore merged into a coherent multi-turn contextual QA set.

C Model Input Example

In this section, we utilize input examples to more clearly illustrate the concepts presented in Sec. 3 of the main paper. We first present input examples for LIVE [5] (corresponding to Sec. 3.1 of the main paper), followed by input examples for our multi-stage training strategy (corresponding to Sec. 3.2 of the main paper). Finally, we will demonstrate Compression Token Insertion and related training details, further elucidating key aspects introduced in Sec. 3.3 of the main paper.

LIVE Input. An input example for the LIVE [5] model is provided below. Visual tokens [F] denote the tokens per frame. The number of visual tokens per frame, |[F]|, is set to 10, comprising 1 CLS token and 3×3 average-pooled spatial tokens for enhanced visual understanding. Tokens marked in purple indicate an output of a_{response}, while green tokens correspond to an output of a_{continue}. Text highlighted in red is subject to language model loss [59, 11, 48], whereas other textual elements receive no supervision. Some chat template strings have been omitted for better visualization.

LIVE Example

[System Prompt]
Observation: [F] [F] ... **User:** Can you tell me where the garbage are when I drop them? **Observation:** [F][F]... [F][F]**Assistant:** The garbage is dropped to the next to the notebook on the counter. **Observation:** [F][F]... [F][F]**Assistant:** The garbage is dropped on the lab bench in front of you. **Observation:** [F] [F] ... **User:** I want to clean them up. **Observation:** [F][F]... [F][F]**Assistant:** You can throw them from the counter and the lab bench into the yellow bucket near the shelf. **Observation:** [F] [F] ...

Stage-1 Input. An input example for the Stage-1 training is provided below. The core distinction from the LIVE [5] example is the transformation of the abrupt supervision signal into a progressive one. Visually, as the purple color deepens, the weight of the supervision signal increases, indicating that the supervision signal becomes stronger as it approaches the optimal response timestamp.

Stage-1 Example

[System Prompt]
Observation: [F] [F] ... **User:** Can you tell me where the garbage are when I drop them? **Observation:** [F][F]... [F]**Assistant:** The garbage is dropped to the next to the notebook on the counter. **Observation:** [F][F]... [F][F]**Assistant:** The garbage is dropped on the lab bench in front of you. **Observation:** [F] [F] ... **User:** I want to clean them up. **Observation:** [F][F]... [F][F][F]**Assistant:** You can throw them from the counter and the lab bench into the yellow bucket near the shelf. **Observation:** [F] [F] ...

Stage-2 Input. First, the set of uncertain timestamps $\mathcal{T}_{\text{uncertain}}$ (shown in Equ. 5) is automatically identified by perceiving timesteps where the model is likely to be confused or uncertain. Specifically, an initial training phase is conducted for one epoch using the $\mathcal{L}_{\text{ask\_high}}(t)$ loss, with $\mathcal{T}_{\text{uncertain}}$ initially set equal to $\mathcal{T}_{\text{interval}}$. An illustrative example is provided below. Compared to Stage 1, the a_{response} is now replaced by $a_{\text{ask\_high}}$, with the blue tokens indicating receiving this new supervision.

[System Prompt]
Observation: [F] [F] ... **User:** Can you tell me where the garbage are when I drop them? **Observation:** [F][F]... [F][HF]**Assistant:** The garbage is dropped to the next to the notebook on the counter. **Observation:** [F][F]... [F][F][HF]**Assistant:** The garbage is dropped on the lab bench in front of you. **Observation:** [F] [F] ... **User:** I want to clean them up. **Observation:** [F][F]... [F][F][F][HF]**Assistant:** You can throw them from the counter and the lab bench into the yellow bucket near the shelf. **Observation:** [F] [F] ...

Subsequently, by comparing the model's predicted sequence against the ground truth sequence, we identify timestamps of erroneous $a_{\text{ask\_high}}$ predictions (t_{error}). For each such error timestamp t_{error}, we locate the nearest preceding timestamp $t_{\text{visual\_change\_prev}}$ characterized by a significant visual feature change, measured using visual [60] similarity. The set $\mathcal{T}_{\text{error}}$ is then defined as the union of intervals $[t_{\text{visual\_change\_prev}}, t_{\text{error}}]$, where for each response turn, t_{error} corresponds to the erroneous prediction with the highest logit if multiple errors are present within that turn. An example is provided below, where red tokens indicate timesteps where the ground truth was a_{continue} but the model erroneously predicted $a_{\text{ask\_high}}$.

[System Prompt]
Observation: [F] [F] . . . **User:** Can you tell me where the garbage are when I drop them? **Observation:** [F][F]. . . [F][F]. . . [F][HF]**Assistant:** The garbage is dropped to the next to the notebook on the counter. **Observation:** [F][F]. . . [F][F]. . . [F][F][HF]**Assistant:** The garbage is dropped on the lab bench in front of you. **Observation:** [F] [F] . . . **User:** I want to clean them up. **Observation:** [F][F]. . . [F][F]. . . [F][F][F][HF]**Assistant:** You can throw them from the counter and the lab bench into the yellow bucket near the shelf. **Observation:** [F] [F] . . .

$\mathcal{T}_{\text{uncertain}}$ is then constructed by merging $\mathcal{T}_{\text{error}}$ with the Ground Truth relevant regions $\mathcal{T}_{\text{interval}}$. This allows the model to learn from mistakes and focus training on challenging moments, encouraging it to utilize scrutiny before making correct decisions in these uncertain scenarios. An illustrative example is provided below.

Stage-2 Example

[System Prompt]
Observation: [F] [F] . . . **User:** Can you tell me where the garbage are when I drop them? **Observation:** [F][F]. . . [F][F][F][F][HF]. . . [F][HF]**Assistant:** The garbage is dropped to the next to the notebook on the counter. **Observation:** [F][F]. . . [F][F][F][F][HF]. . . [F][F][HF]**Assistant:** The garbage is dropped on the lab bench in front of you. **Observation:** [F] [F] . . . **User:** I want to clean them up. **Observation:** [F][F]. . . [F][F]. . . [F][F][F][HF]**Assistant:** You can throw them from the counter and the lab bench into the yellow bucket near the shelf. **Observation:** [F] [F] . . .

Proactive Dynamic Compression Mechanism Example. An example illustrating the insertion of compression tokens is provided below. Compared to the Stage-2 example, $\langle\text{ct}\rangle$ tokens are inserted after segments of input, specifically following multiple low-resolution frames, single high-resolution frames, and text replies.

Compression Example

[System Prompt]
Observation: [F] [F] . . . $\langle\text{ct}\rangle$ **User:** Can you tell me where the garbage are when I drop them? **Observation:** [F][F]. . . [F][F][F]$\langle\text{ct}\rangle$ [HF]$\langle\text{ct}\rangle$ . . . [F]$\langle\text{ct}\rangle$ [HF]$\langle\text{ct}\rangle$ **Assistant:** The garbage is dropped to the next to the notebook on the counter. $\langle\text{ct}\rangle$ **Observation:** [F][F]. . . [F][F][F][F]$\langle\text{ct}\rangle$ [HF]$\langle\text{ct}\rangle$ . . . [F][F]$\langle\text{ct}\rangle$ [HF]$\langle\text{ct}\rangle$ **Assistant:** The garbage is dropped on the lab bench in front of you. $\langle\text{ct}\rangle$ **Observation:** [F] [F] . . . $\langle\text{ct}\rangle$ **User:** I want to clean them up. **Observation:** [F][F]. . . [F][F]$\langle\text{ct}\rangle$ [HF]$\langle\text{ct}\rangle$ . . . [F][F]$\langle\text{ct}\rangle$ [F][HF]$\langle\text{ct}\rangle$ **Assistant:** You can throw them from the counter and the lab bench into the yellow bucket near the shelf. $\langle\text{ct}\rangle$ **Observation:** [F] [F] . . .

During training, inspired by [43], the LLM is trained to process response turns sequentially.The initial sequence provided to the LLM is as follows:

[System Prompt]
Observation: [F] [F] . . . $\langle\text{ct}\rangle$

Past visual tokens are compressed into a $\langle\text{ct}\rangle$. The System Prompt, containing essential system-level instructions [53], remains uncompressed. The subsequent sequence processed by the LLM is as follows, where gray portions indicate tokens stored in the KV Cache:

		Stage-1	Stage-2	Stage-3
Data	Dataset	Ego4D: Narration Stream + GoalStep Stream ESTP-IT Single-Turn + Multi-Turn	ESTP-IT Single-Turn + Multi-Turn	ESTP-IT Multi-Turn
	#Samples	113K + 21K 60K + 20K	60K + 20K	20K
Model	Base LLM	LLaMA3	LLaMA3	LLaMA3
	Vision Encoder(s)	SigLIP	SigLIP	SigLIP
	Vision Token per Frame	1+3x3	Low Res: 1+3x3 High Res: 1+7x7	Low Res: 1+3x3 High Res: 1+7x7
	Connector	MLP	MLP	MLP
	Trainable	Connector(full) LLM(LoRA r=128, scale=256)	Connector(full) LLM(LoRA r=128, scale=256)	Connector(full) LLM(LoRA r=128, scale=256)
Initialization	Connector	N/A	Stage-1 Connector	Stage-2 Connector
	LLM	LLaMA3	+ Stage-1 LoRA	+ Stage-2 LoRA
Training	Batch Size per Device	1	1	1
	Gradient Accumulation	8	8	8
	Learning Rate	2e-4	1e-4	5e-5
	Warm-up Ratio	0.05	0.05	0.05
	LR Scheduler	Cosine	Cosine	Cosine
	Optimizer	Adamw	Adamw	Adamw
	Epochs	2	1	1
	Precision	bf16 fp16	bf16 fp16	bf16 fp16

Table 6: Multi-Stage Training Plan in ESTP

[System Prompt] $\langle \mathrm{ct} \rangle$
User: Can you tell me where the garbage are when I drop them? **Observation:** [F][F]...[F][F][F]$\langle \mathrm{ct} \rangle$ [HF]$\langle \mathrm{ct} \rangle$ ...[F]$\langle \mathrm{ct} \rangle$ [HF]$\langle \mathrm{ct} \rangle$ **Assistant:** The garbage is dropped to the next to the notebook on the counter. $\langle \mathrm{ct} \rangle$

Following this, solely the user's query content and the $\langle \mathrm{ct} \rangle$ are maintained in the KV cache.

D Training Implementation Detail

In this section, we provide detailed implementation configurations of our training methodology.

ESTP-Bench. Our training methodology employs a three-stage strategy to progressively endow the VideoLLM-EyeWO model with advanced proactive capabilities. Tab. 6 summarizes key details of each stage's specific configuration and learning objectives, while Tab. 5 presents the corresponding ablation results.

COIN-Benchmark. Tab. 7 presents the training plan on the COIN [46] dataset. For a fair comparison with VideoLLM-Online [5], we utilized the same base model (LlaMa3 [16] and SigLIP [60]) and adopted identical training hyperparameters.

E ESTP-Bench Evaluation Details

In this section, we first present the parameter scales and hyperparameters for various models. Subsequently, we illustrate the corresponding prompts used in the evaluation.

E.1 Various MLLMs Hyperparameter

For Offline MLLMs, considering Synchronized Efficiency, we employed models around the 7B/8B scale. For the Response-in-Last strategy, a single query was issued after processing the complete video segment. Regarding the Polling strategy, the querying frequency was set to 0.175 queries per second. This frequency was chosen to match the model's response efficiency (Action Per Second), as illustrated in Fig. 7. Given that our videos are often significantly longer than the typical input frame capacity of these MLLMs, we followed the open-source code from [27], utilizing the corresponding sampling frequencies or input frame counts for different models.

Data	Dataset	COIN
Model	Base LLM Vision Encoder(s) Vision Token per Frame Connector Trainable	LLaMA3 SigLIP Low Res: 1+3x3 High Res: 1+7x7 MLP Connector(full) LLM(LoRA r=128, scale=256)
Initialization	Connector LLM	N/A LLaMA3
Training	Batch Size per Device Gradient Accumulation Learning Rate Warm-up Ratio LR Scheduler Optimizer Epochs Precision	1 8 1.5e-4 0.05 Cosine Adamw 5 bf16 fp16

Table 7: Training Plan in COIN [46]

Model	**Params**	**Frame**	**Query Frequency**
Offline MLLMs Response-in-Last			
LLaVA-OneVision	7B	32	Ask per Question
Qwen2-VL	8B	0.2-1 fps	Ask per Question
MiniCPM-V	8B	64	Ask per Question
LLaVA-NeXT-Video	7B	32	Ask per Question
InternVL-V2	8B	32	Ask per Question
VLMs for Streaming Detection			
CLIP	Base	1 fps	1 Hz
LaViLa	Base	1 fps	1 Hz
EgoVLP	Base	1 fps	1 Hz
Offline MLLMs Polling Strategy			
LLaVA-OneVision	7B	32	0.175 Hz
Qwen2-VL	8B	0.2-1 fps	0.175 Hz
MiniCPM-V	8B	64	0.175 Hz
LLaVA-NeXT-Video	7B	32	0.175 Hz
InternVL-V2	8B	32	0.175 Hz
Online MLLMs			
LIVE(threshold=0.8)	8B	2 fps	2 Hz
LIVE(threshold=0.9)	8B	2 fps	2 Hz
MMDuet	8B	2 fps	2 Hz
VideoLLM-EyeWO(Ours)	8B	2 fps	2 Hz

Table 8: Parameter Scales and Hyperparameters for Various Models

For VLMs, we adopted model parameters and input sampling frequencies consistent with [13]. Given their inherent lack of text generation capabilities and consequently, their relatively low computational cost, the query frequency was set to match the input sampling frequency.

For Online MLLMs, we utilized model parameters, input frequencies, and query frequencies as reported in [5, 51].

E.2 Evalutation Prompt

Below, we present the prompt used for the Offline MLLMs Response-in-Last strategy. Inspired by [37], we guided the model within the system prompt to output all answers corresponding to a given question, along with their respective frame indices. These frame indices are then converted into corresponding timestamps via a defined sampling relationship. Contextual information, encompassing both timestamps and content, is incorporated into the prompt following the approach of [27].

Below, we present the prompt used for the Offline MLLMs Polling Strategy, following the approach of [27]. The sole distinction lies in that proactive tasks in [27] solely require the model to judge if it can answer a question at the current moment, outputting only 'yes' or 'no'. In contrast, our approach additionally requires the model to generate a textual reply. Therefore, at timesteps where the model indicates readiness (by outputting 'yes'), we execute an additional query, prompting the model to generate the answer.

Prompt Used for Response-in-Last

```
You are an advanced video AI assistant. Given a video and a question, carefully
analyze each frame of the video, identify all relevant moments that help answer
the question, and provide the corresponding frame numbers along with the answer.
The format should be: '[frame idx] answer'.
For example, [6] The object is a cup.
[60] The object is a cup.
[100] The object is a yellow cup.
```

Here are the contextual information related to the video. Please answer the questions based on the contextual information:
At timestamp {}, the following question occurred: {}
At timestamp {}, the following answer occurred: {}

Here is the question. Answer it and don't confuse it with the previous conversation
Question: {}
The answer is:

Prompt Used for Polling Strategy

```
You are an advanced video question-answering AI assistant. You have been
provided with video and a question related to the video. Your task is to
carefully analyze the video and provide the answer to the question. You need
to carefully confirm whether the video content meet the conditions of the
question, and then output the correct content.
```

Here are the contextual information related to the video. Please answer the questions based on the contextual information:
At timestamp {}, the following question occurred: {}
At timestamp {}, the following answer occurred: {}

Here is the question. Answer it and don't confuse it with the previous conversation
Question: Is it the right time to answer the question "{}"? You need to answer yes or no. / Please answer the question: "{}"
The answer is:

F Limitation and Future Work

To build a truly intelligent agent akin to Jarvis, it is essential to move beyond passive perception and incorporate active interaction with the environment. In this work, we focus on a constrained setting where the agent operates solely on pre-recorded videos. The objective is to train a model that can perceive the visual world and respond promptly within a fixed observation window. While this setting enables us to study perceptual grounding and response capabilities in a controlled manner, it inevitably limits the agent's ability to engage in real-time decision making, action planning, or closed-loop interaction.

This limitation highlights an important future direction: extending perceptual agents into embodied settings where they can interact with the environment through physical actions. For instance, integrating vision-language models into real-world robots-such as home assistants, warehouse manipulators, or autonomous drones—would require the ability to reason about action consequences, update beliefs based on new observations, and adapt behavior on the fly. Existing platforms like Habitat [32, 40, 45] for embodied AI or Meta's HomeAssist offer promising testbeds for such developments.

Therefore, future work should explore how to bridge the gap between static visual perception and dynamic agent-environment interaction. This includes developing methods for real-time perception-action loops, task-aware decision making, and cross-modal alignment under continual feedback. Strengthening interaction with the environment is a crucial step toward building general-purpose, autonomous agents that go beyond observation to perform useful actions in the real world.

G Data Examples

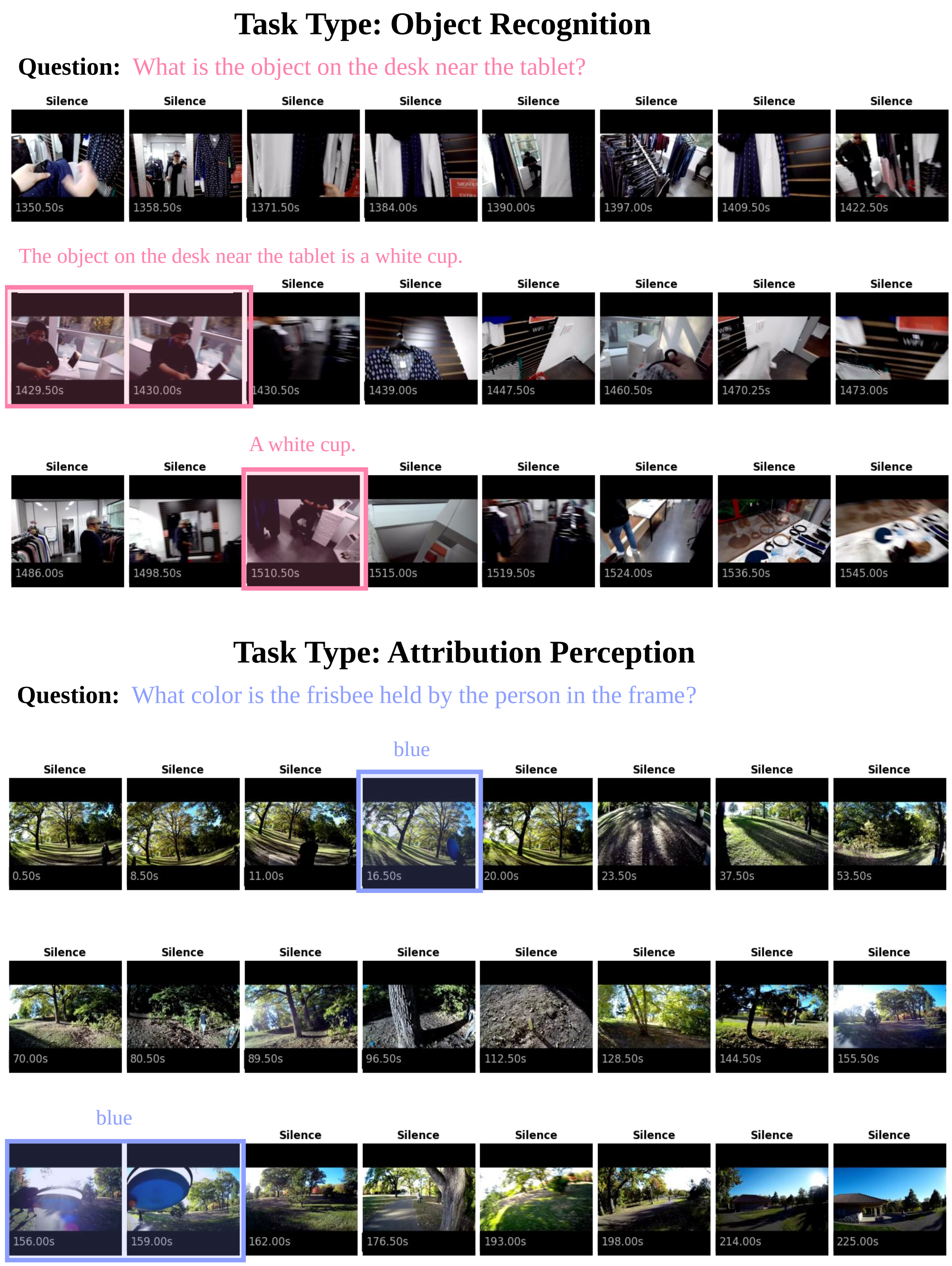

Figure 10: Data examples for Object Recognition, Attribution Perception tasks.

Task Type: Text-Rich Understanding

Question: Can you remind me of the specific brand name written on the signboard above the store entrance?

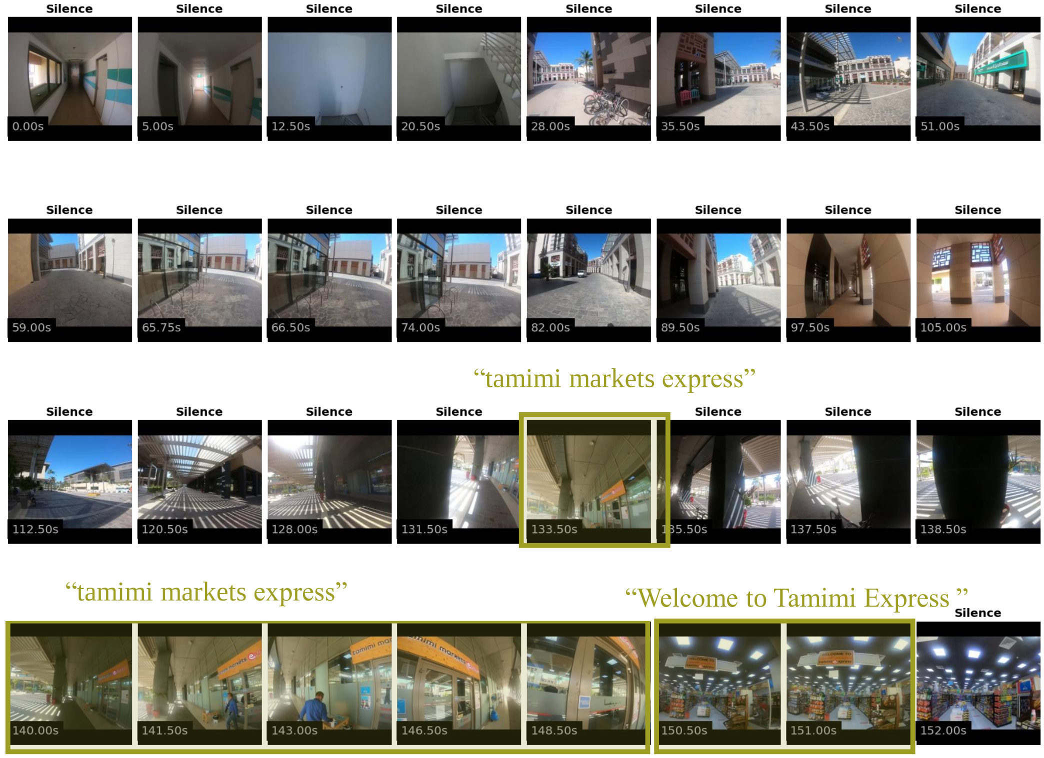

Task Type: Object Location

Question: Where's the blue bike's position in the room?

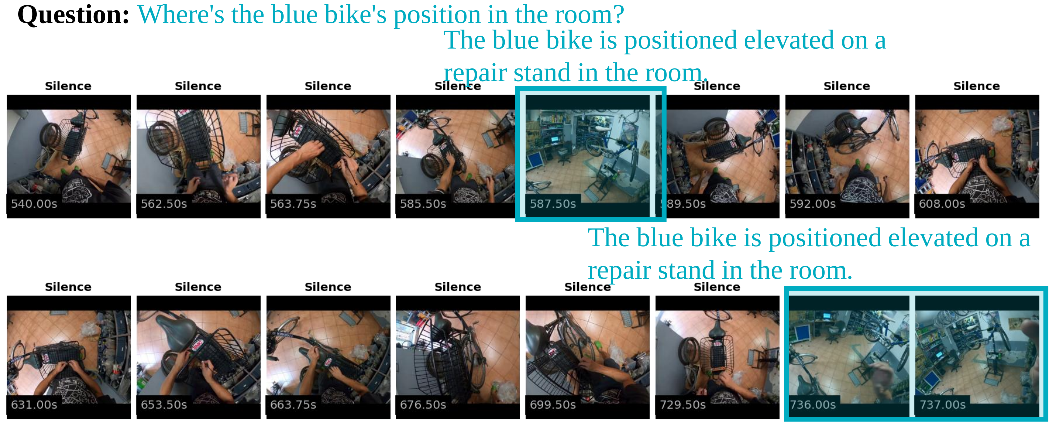

Figure 11: Data examples for Text-Rich Understanding, Object Location tasks.

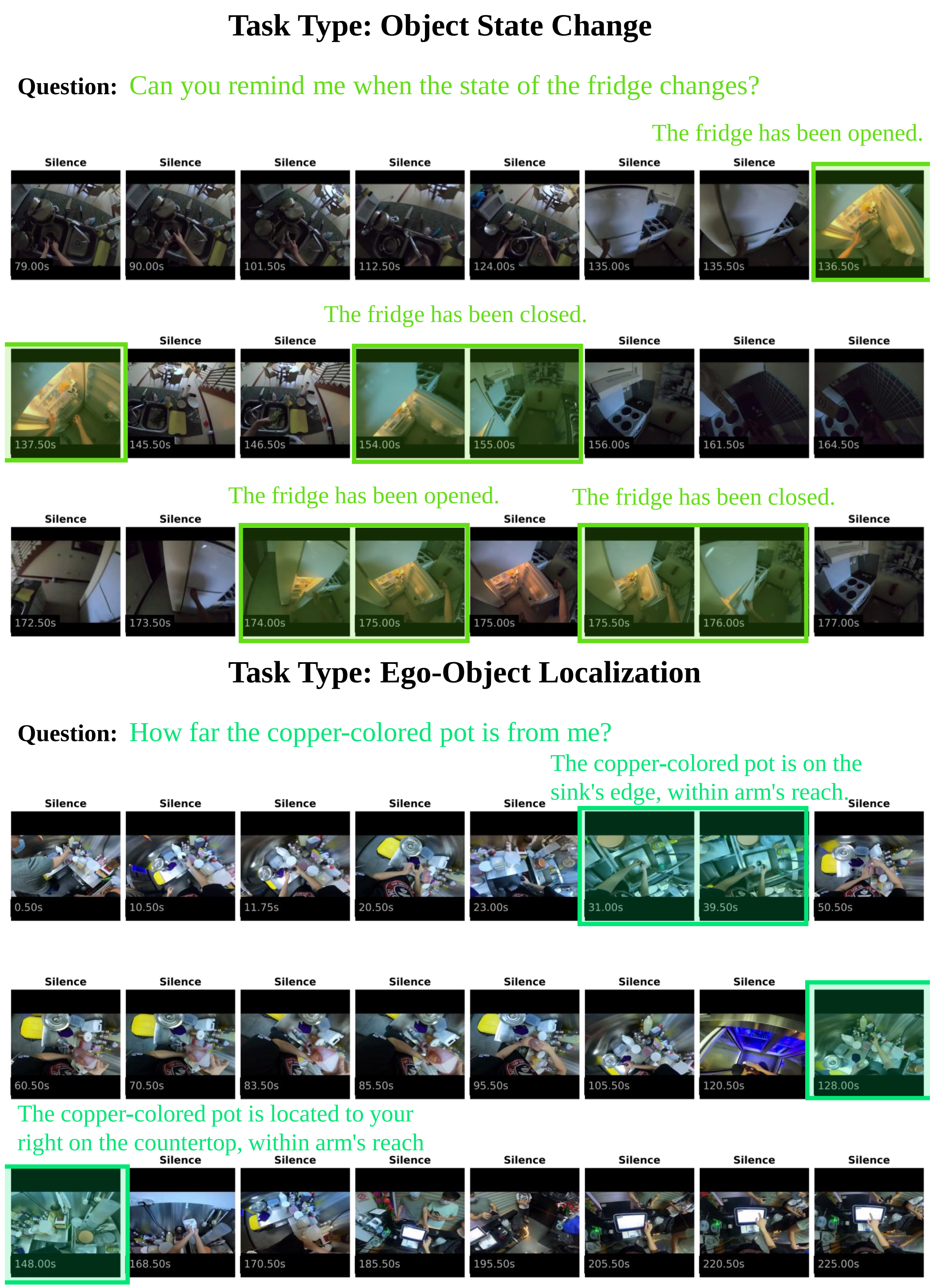

Figure 12: Data examples for Object State Change, Ego-Object Localization tasks.

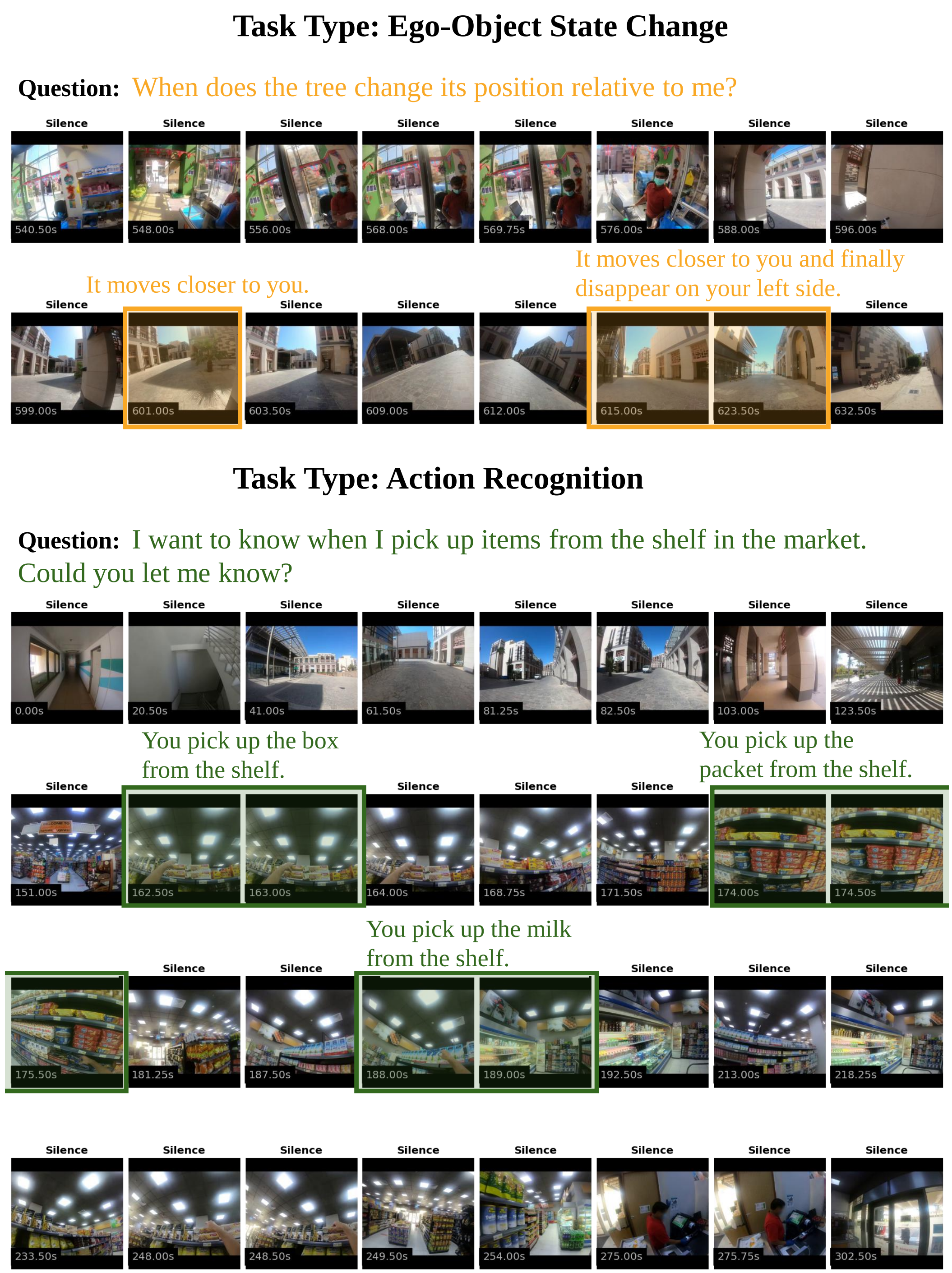

Figure 13: Data examples for Ego-Object State Change, Action Recognition tasks.

Figure 14: Data examples for Object Function, Information Function tasks.

Task Type: Task Understanding

Question: Please explain how to achieve my goal of seasoning vegetables, starting from the very beginning and detailing each step.

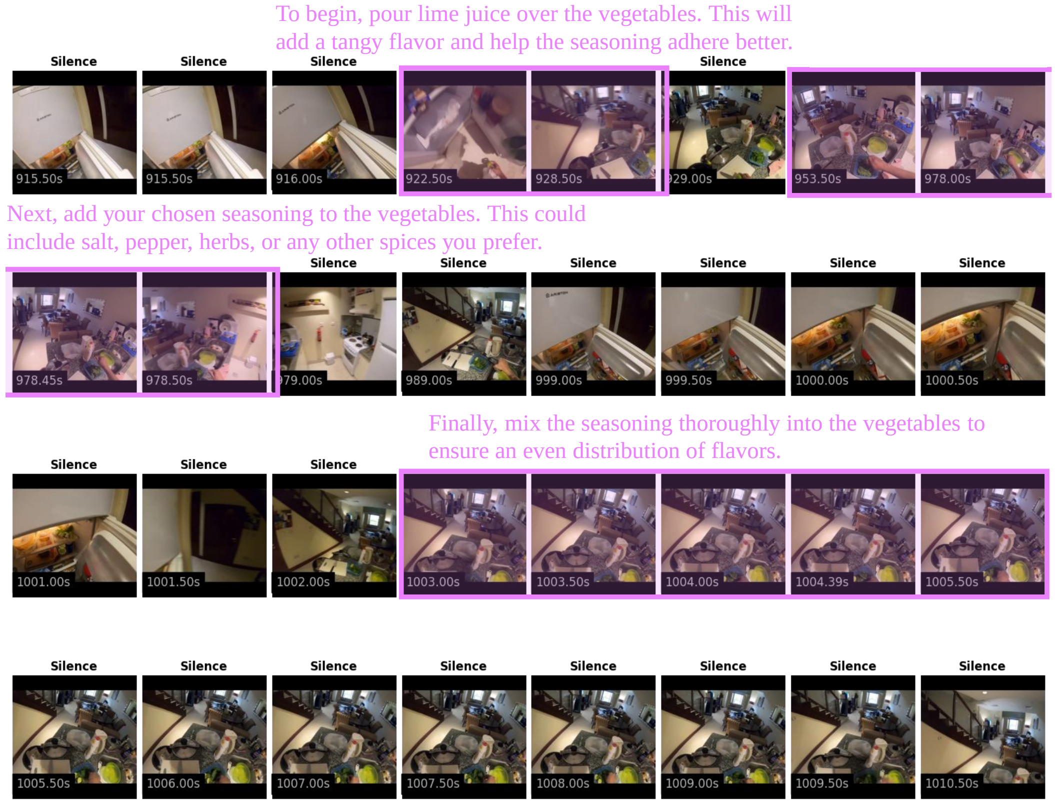

Task Type: Next Action Reasoning

Question: What should I do next to continue dicing ingredients after completing the earlier tasks: washing utensils and slicing meat? Please provide clear instructions

Figure 15: Data examples for Task Understanding, Next Action Reasoning tasks.

Task Type: Object Relative Context

Question: [270s] Could you remind me when the dog is pooing?

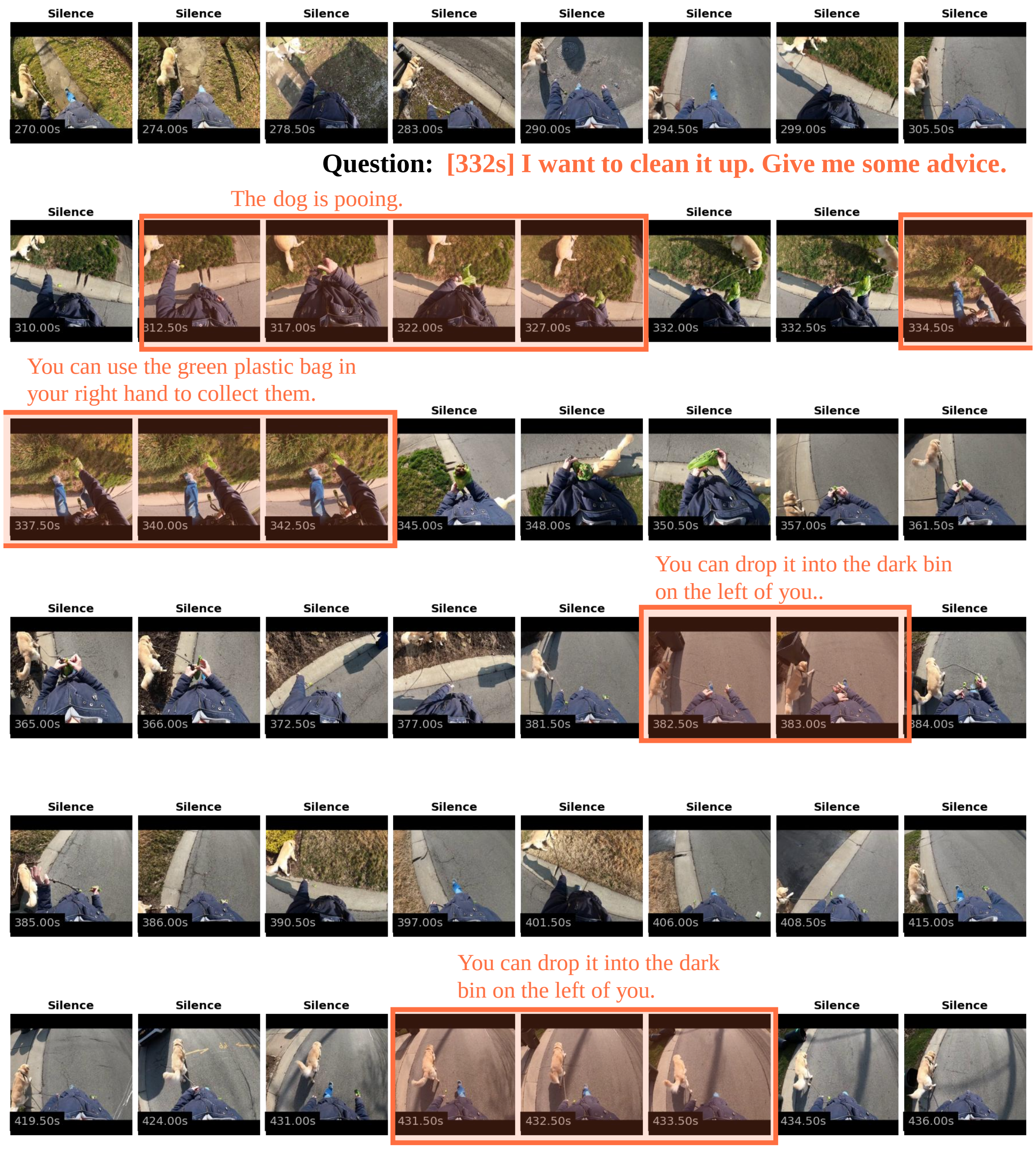

Figure 16: Data examples for Object Relative Context task.

Task Type: Object Relative Context

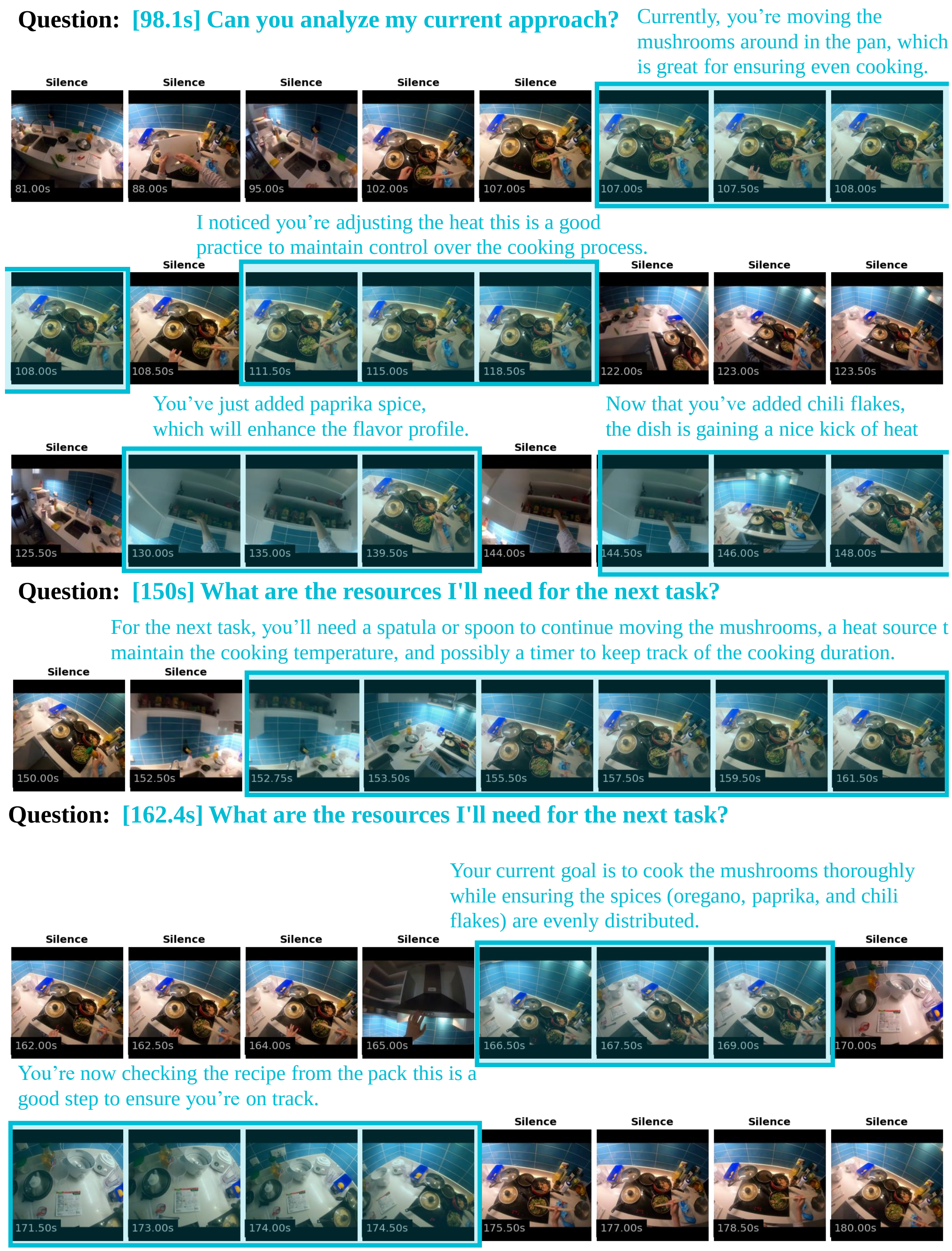

Figure 17: Data examples for Task Relative Context task.

H Qualitative Results

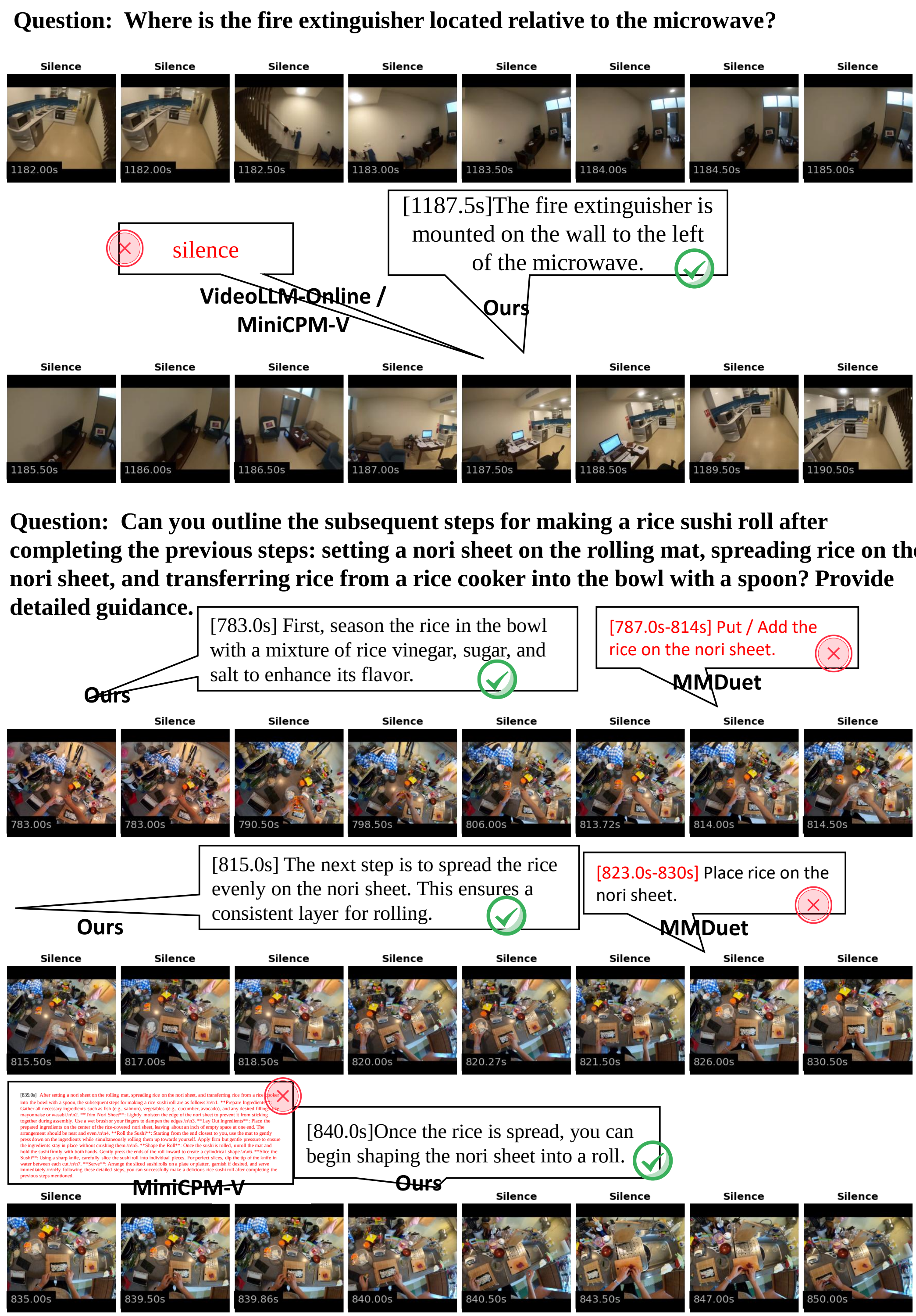

Figure 18: Qualitative Comparison with Baseline.

Question: What can help in case of fire?

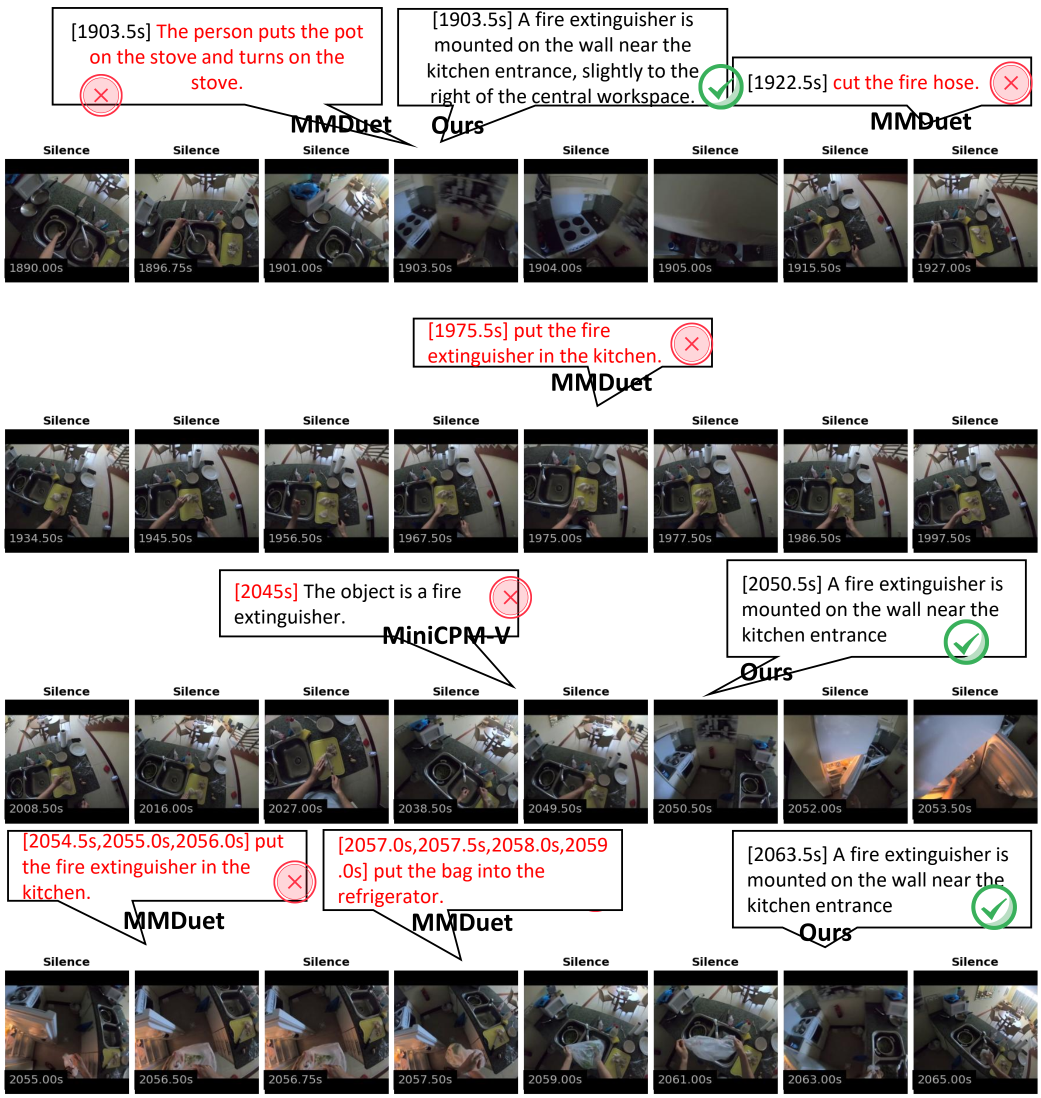

Figure 19: Qualitative Comparison with Baseline.

References

[1] Kirolos Ataallah, Eslam Abdelrahman, Mahmoud Ahmed, Chenhui Gou, Khushbu Pahwa, Jian Ding, and Mohamed Elhoseiny. Infinibench: A benchmark for large multi-modal models in long-form movies and tv shows, 2025.

[2] Siddhant Bansal, Michael Wray, and Dima Damen. Hoi-ref: Hand-object interaction referral in egocentric vision, 2024.

[3] Leonard Bärmann and Alex Waibel. Where did i leave my keys? — episodic-memory-based question answering on egocentric videos. In *2022 IEEE/CVF Conference on Computer Vision and Pattern Recognition Workshops (CVPRW)*, pages 1559–1567, 2024. ISSN: 2160-7516.

[4] Jieneng Chen, Luoxin Ye, Ju He, Zhao-Yang Wang, Daniel Khashabi, and Alan Yuille. Efficient large multi-modal models via visual context compression, 2024.

[5] Joya Chen, Zhaoyang Lv, Shiwei Wu, Kevin Qinghong Lin, Chenan Song, Difei Gao, Jia-Wei Liu, Ziteng Gao, Dongxing Mao, and Mike Zheng Shou. Videollm-online: Online video large language model for streaming video, 2024.

[6] Yi Chen, Yuying Ge, Yixiao Ge, Mingyu Ding, Bohao Li, Rui Wang, Ruifeng Xu, Ying Shan, and Xihui Liu. Egoplan-bench: Benchmarking multimodal large language models for human-level planning, 2024.

[7] Zhe Chen, Weiyun Wang, Hao Tian, Shenglong Ye, Zhangwei Gao, Erfei Cui, Wenwen Tong, Kongzhi Hu, Jiapeng Luo, Zheng Ma, Ji Ma, Jiaqi Wang, Xiaoyi Dong, Hang Yan, Hewei Guo, Conghui He, Botian Shi, Zhenjiang Jin, Chao Xu, Bin Wang, Xingjian Wei, Wei Li, Wenjian Zhang, Bo Zhang, Pinlong Cai, Licheng Wen, Xiangchao Yan, Min Dou, Lewei Lu, Xizhou Zhu, Tong Lu, Dahua Lin, Yu Qiao, Jifeng Dai, and Wenhai Wang. How far are we to gpt-4v? closing the gap to commercial multimodal models with open-source suites, 2024.

[8] Sijie Cheng, Kechen Fang, Yangyang Yu, Sicheng Zhou, Bohao Li, Ye Tian, Tingguang Li, Lei Han, and Yang Liu. Videgothink: Assessing egocentric video understanding capabilities for embodied ai, 2024.

[9] Dima Damen, Hazel Doughty, Giovanni Maria Farinella, Sanja Fidler, Antonino Furnari, Evangelos Kazakos, Davide Moltisanti, Jonathan Munro, Toby Perrett, Will Price, and Michael Wray. Scaling egocentric vision: The epic-kitchens dataset, 2018.

[10] DeepSeek-AI, Aixin Liu, Bei Feng, Bing Xue, Bingxuan Wang, Bochao Wu, Chengda Lu, Chenggang Zhao, Chengqi Deng, Chenyu Zhang, Chong Ruan, Damai Dai, Daya Guo, Dejian Yang, Deli Chen, Dongjie Ji, Erhang Li, Fangyun Lin, Fucong Dai, Fuli Luo, Guangbo Hao, Guanting Chen, Guowei Li, H. Zhang, Han Bao, Hanwei Xu, Haocheng Wang, Haowei Zhang, Honghui Ding, Huajian Xin, Huazuo Gao, Hui Li, Hui Qu, J. L. Cai, Jian Liang, Jianzhong Guo, Jiaqi Ni, Jiashi Li, Jiawei Wang, Jin Chen, Jingchang Chen, Jingyang Yuan, Junjie Qiu, Junlong Li, Junxiao Song, Kai Dong, Kai Hu, Kaige Gao, Kang Guan, Kexin Huang, Kuai Yu, Lean Wang, Lecong Zhang, Lei Xu, Leyi Xia, Liang Zhao, Litong Wang, Liyue Zhang, Meng Li, Miaojun Wang, Mingchuan Zhang, Minghua Zhang, Minghui Tang, Mingming Li, Ning Tian, Panpan Huang, Peiyi Wang, Peng Zhang, Qiancheng Wang, Qihao Zhu, Qinyu Chen, Qiushi Du, R. J. Chen, R. L. Jin, Ruiqi Ge, Ruisong Zhang, Ruizhe Pan, Runji Wang, Runxin Xu, Ruoyu Zhang, Ruyi Chen, S. S. Li, Shanghao Lu, Shangyan Zhou, Shanhuang Chen, Shaoqing Wu, Shengfeng Ye, Shengfeng Ye, Shirong Ma, Shiyu Wang, Shuang Zhou, Shuiping Yu, Shunfeng Zhou, Shuting Pan, T. Wang, Tao Yun, Tian Pei, Tianyu Sun, W. L. Xiao, Wangding Zeng, Wanjia Zhao, Wei An, Wen Liu, Wenfeng Liang, Wenjun Gao, Wenqin Yu, Wentao Zhang, X. Q. Li, Xiangyue Jin, Xianzu Wang, Xiao Bi, Xiaodong Liu, Xiaohan Wang, Xiaojin Shen, Xiaokang Chen, Xiaokang Zhang, Xiaosha Chen, Xiaotao Nie, Xiaowen Sun, Xiaoxiang Wang, Xin Cheng, Xin Liu, Xin Xie, Xingchao Liu, Xingkai Yu, Xinnan Song, Xinxia Shan, Xinyi Zhou, Xinyu Yang, Xinyuan Li, Xuecheng Su, Xuheng Lin, Y. K. Li, Y. Q. Wang, Y. X. Wei, Y. X. Zhu, Yang Zhang, Yanhong Xu, Yanhong Xu, Yanping Huang, Yao Li, Yao Zhao, Yaofeng Sun, Yaohui Li, Yaohui Wang, Yi Yu, Yi Zheng, Yichao Zhang, Yifan Shi, Yiliang Xiong, Ying He, Ying Tang, Yishi Piao, Yisong Wang, Yixuan Tan, Yiyang Ma, Yiyuan Liu, Yongqiang Guo, Yu Wu, Yuan Ou, Yuchen Zhu, Yuduan Wang, Yue Gong, Yuheng Zou, Yujia He, Yukun Zha, Yunfan Xiong, Yunxian Ma, Yuting Yan, Yuxiang Luo, Yuxiang You, Yuxuan Liu, Yuyang Zhou, Z. F. Wu, Z. Z. Ren, Zehui Ren, Zhangli Sha, Zhe Fu, Zhean Xu, Zhen Huang, Zhen Zhang, Zhenda Xie, Zhengyan Zhang, Zhewen Hao, Zhibin Gou, Zhicheng Ma, Zhigang Yan, Zhihong Shao, Zhipeng Xu, Zhiyu Wu, Zhongyu Zhang, Zhuoshu Li, Zihui Gu, Zijia Zhu, Zijun Liu, Zilin Li, Ziwei Xie, Ziyang Song, Ziyi Gao, and Zizheng Pan. Deepseek-v3 technical report, 2025.

[11] Jacob Devlin, Ming-Wei Chang, Kenton Lee, and Kristina Toutanova. Bert: Pre-training of deep bidirectional transformers for language understanding, 2019.

[12] Shangzhe Di, Zhelun Yu, Guanghao Zhang, Haoyuan Li, Hao Cheng, Bolin Li, Wanggui He, Fangxun Shu, Hao Jiang, et al. Streaming video question-answering with in-context video kv-cache retrieval. In *ICLR*, 2025.

[13] Cristobal Eyzaguirre, Eric Tang, Shyamal Buch, Adrien Gaidon, Jiajun Wu, and Juan Carlos Niebles. Streaming detection of queried event start, 2024.

[14] Chaoyou Fu, Yuhan Dai, Yongdong Luo, Lei Li, Shuhuai Ren, Renrui Zhang, Zihan Wang, Chenyu Zhou, Yunhang Shen, Mengdan Zhang, Peixian Chen, Yanwei Li, Shaohui Lin, Sirui Zhao, Ke Li, Tong Xu, Xiawu Zheng, Enhong Chen, Caifeng Shan, Ran He, and Xing Sun. Video-mme: The first-ever comprehensive evaluation benchmark of multi-modal llms in video analysis, 2025.

[15] Gabriele Goletto, Tushar Nagarajan, Giuseppe Averta, and Dima Damen. Amego: Active memory from long egocentric videos, 2024.

[16] Aaron Grattafiori, Abhimanyu Dubey, Abhinav Jauhri, Abhinav Pandey, Abhishek Kadian, Ahmad Al-Dahle, Aiesha Letman, Akhil Mathur, Alan Schelten, Alex Vaughan, Amy Yang, Angela Fan, Anirudh Goyal, Anthony Hartshorn, Aobo Yang, Archi Mitra, Archie Sravankumar, Artem Korenev, Arthur Hinsvark, Arun Rao, Aston Zhang, Aurelien Rodriguez, Austen Gregerson, Ava Spataru, Baptiste Roziere, Bethany Biron, Binh Tang, Bobbie Chern, Charlotte Caucheteux, Chaya Nayak, Chloe Bi, Chris Marra, Chris McConnell, Christian Keller, Christophe Touret, Chunyang Wu, Corinne Wong, Cristian Canton Ferrer, Cyrus Nikolaidis, Damien Allonsius, Daniel Song, Danielle Pintz, Danny Livshits, Danny Wyatt, David Esiobu, Dhruv Choudhary, Dhruv Mahajan, Diego Garcia-Olano, Diego Perino, Dieuwke Hupkes, Egor Lakomkin, Ehab AlBadawy, Elina Lobanova, Emily Dinan, Eric Michael Smith, Filip Radenovic, Francisco Guzmán, Frank Zhang, Gabriel Synnaeve, Gabrielle Lee, Georgia Lewis Anderson, Govind Thattai, Graeme Nail, Gregoire Mialon, Guan Pang, Guillem Cucurell, Hailey Nguyen, Hannah Korevaar, Hu Xu, Hugo Touvron, Iliyan Zarov, Imanol Arrieta Ibarra, Isabel Kloumann, Ishan Misra, Ivan Evtimov, Jack Zhang, Jade Copet, Jaewon Lee, Jan Geffert, Jana Vranes, Jason Park, Jay Mahadeokar, Jeet Shah, Jelmer van der Linde, Jennifer Billock, Jenny Hong, Jenya Lee, Jeremy Fu, Jianfeng Chi, Jianyu Huang, Jiawen Liu, Jie Wang, Jiecao Yu, Joanna Bitton, Joe Spisak, Jongsoo Park, Joseph Rocca, Joshua Johnstun, Joshua Saxe, Junteng Jia, Kalyan Vasuden Alwala, Karthik Prasad, Kartikeya Upasani, Kate Plawiak, Ke Li, Kenneth Heafield, Kevin Stone, Khalid El-Arini, Krithika Iyer, Kshitiz Malik, Kuenley Chiu, Kunal Bhalla, Kushal Lakhotia, Lauren Rantala-Yeary, Laurens van der Maaten, Lawrence Chen, Liang Tan, Liz Jenkins, Louis Martin, Lovish Madaan, Lubo Malo, Lukas Blecher, Lukas Landzaat, Luke de Oliveira, Madeline Muzzi, Mahesh Pasupuleti, Mannat Singh, Manohar Paluri, Marcin Kardas, Maria Tsimpoukelli, Mathew Oldham, Mathieu Rita, Maya Pavlova, Melanie Kambadur, Mike Lewis, Min Si, Mitesh Kumar Singh, Mona Hassan, Naman Goyal, Narjes Torabi, Nikolay Bashlykov, Nikolay Bogoychev, Niladri Chatterji, Ning Zhang, Olivier Duchenne, Onur Çelebi, Patrick Alrassy, Pengchuan Zhang, Pengwei Li, Petar Vasic, Peter Weng, Prajjwal Bhargava, Pratik Dubal, Praveen Krishnan, Punit Singh Koura, Puxin Xu, Qing He, Qingxiao Dong, Ragavan Srinivasan, Raj Ganapathy, Ramon Calderer, Ricardo Silveira Cabral, Robert Stojnic, Roberta Raileanu, Rohan Maheswari, Rohit Girdhar, Rohit Patel, Romain Sauvestre, Ronnie Polidoro, Roshan Sumbaly, Ross Taylor, Ruan Silva, Rui Hou, Rui Wang, Saghar Hosseini, Sahana Chennabasappa, Sanjay Singh, Sean Bell, Seohyun Sonia Kim, Sergey Edunov, Shaoliang Nie, Sharan Narang, Sharath Raparthy, Sheng Shen, Shengye Wan, Shruti Bhosale, Shun Zhang, Simon Vandenhende, Soumya Batra, Spencer Whitman, Sten Sootla, Stephane Collot, Suchin Gururangan, Sydney Borodinsky, Tamar Herman, Tara Fowler, Tarek Sheasha, Thomas Georgiou, Thomas Scialom, Tobias Speckbacher, Todor Mihaylov, Tong Xiao, Ujjwal Karn, Vedanuj Goswami, Vibhor Gupta, Vignesh Ramanathan, Viktor Kerkez, Vincent Gonguet, Virginie Do, Vish Vogeti, Vítor Albiero, Vladan Petrovic, Weiwei Chu, Wenhan Xiong, Wenyin Fu, Whitney Meers, Xavier Martinet, Xiaodong Wang, Xiaofang Wang, Xiaoqing Ellen Tan, Xide Xia, Xinfeng Xie, Xuchao Jia, Xuewei Wang, Yaelle Goldschlag, Yashesh Gaur, Yasmine Babaei, Yi Wen, Yiwen Song, Yuchen Zhang, Yue Li, Yuning Mao, Zacharie Delpierre Coudert, Zheng Yan, Zhengxing Chen, Zoe Papakipos, Aaditya Singh, Aayushi Srivastava, Abha Jain, Adam Kelsey, Adam Shajnfeld, Adithya Gangidi, Adolfo Victoria, Ahuva Goldstand, Ajay Menon, Ajay Sharma, Alex Boesenberg, Alexei Baevski, Allie Feinstein, Amanda Kallet, Amit Sangani, Amos Teo, Anam Yunus, Andrei Lupu, Andres Alvarado, Andrew Caples, Andrew Gu, Andrew Ho, Andrew Poulton, Andrew Ryan, Ankit Ramchandani, Annie Dong, Annie Franco, Anuj Goyal, Aparajita Saraf, Arkabandhu Chowdhury, Ashley Gabriel, Ashwin Bharambe, Assaf Eisenman, Azadeh Yazdan, Beau James, Ben Maurer, Benjamin Leonhardi, Bernie Huang, Beth Loyd, Beto De Paola, Bhargavi Paranjape, Bing Liu, Bo Wu, Boyu Ni, Braden Hancock, Bram Wasti, Brandon Spence, Brani Stojkovic, Brian Gamido, Britt Montalvo, Carl Parker, Carly Burton, Catalina Mejia, Ce Liu, Changhan Wang, Changkyu Kim, Chao Zhou, Chester Hu, Ching-Hsiang Chu, Chris Cai, Chris Tindal, Christoph Feichtenhofer, Cynthia Gao, Damon Civin, Dana Beaty, Daniel Kreymer, Daniel Li, David Adkins, David Xu, Davide Testuggine, Delia David, Devi Parikh, Diana Liskovich, Didem Foss, Dingkang Wang, Duc Le, Dustin Holland, Edward Dowling, Eissa Jamil, Elaine Montgomery, Eleonora Presani, Emily Hahn, Emily Wood, Eric-Tuan Le, Erik Brinkman, Esteban Arcaute, Evan Dunbar, Evan Smothers, Fei Sun, Felix Kreuk, Feng Tian, Filippos Kokkinos, Firat Ozgenel, Francesco Caggioni, Frank Kanayet, Frank Seide, Gabriela Medina Florez, Gabriella

Schwarz, Gada Badeer, Georgia Swee, Gil Halpern, Grant Herman, Grigory Sizov, Guangyi, Zhang, Guna Lakshminarayanan, Hakan Inan, Hamid Shojanazeri, Han Zou, Hannah Wang, Hanwen Zha, Haroun Habeeb, Harrison Rudolph, Helen Suk, Henry Aspegren, Hunter Goldman, Hongyuan Zhan, Ibrahim Damlaj, Igor Molybog, Igor Tufanov, Ilias Leontiadis, Irina-Elena Veliche, Itai Gat, Jake Weissman, James Geboski, James Kohli, Janice Lam, Japhet Asher, Jean-Baptiste Gaya, Jeff Marcus, Jeff Tang, Jennifer Chan, Jenny Zhen, Jeremy Reizenstein, Jeremy Teboul, Jessica Zhong, Jian Jin, Jingyi Yang, Joe Cummings, Jon Carvill, Jon Shepard, Jonathan McPhie, Jonathan Torres, Josh Ginsburg, Junjie Wang, Kai Wu, Kam Hou U, Karan Saxena, Kartikay Khandelwal, Katayoun Zand, Kathy Matosich, Kaushik Veeraraghavan, Kelly Michelena, Keqian Li, Kiran Jagadeesh, Kun Huang, Kunal Chawla, Kyle Huang, Lailin Chen, Lakshya Garg, Lavender A, Leandro Silva, Lee Bell, Lei Zhang, Liangpeng Guo, Licheng Yu, Liron Moshkovich, Luca Wehrstedt, Madian Khabsa, Manav Avalani, Manish Bhatt, Martynas Mankus, Matan Hasson, Matthew Lennie, Matthias Reso, Maxim Groshev, Maxim Naumov, Maya Lathi, Meghan Keneally, Miao Liu, Michael L. Seltzer, Michal Valko, Michelle Restrepo, Mihir Patel, Mik Vyatskov, Mikayel Samvelyan, Mike Clark, Mike Macey, Mike Wang, Miquel Jubert Hermoso, Mo Metanat, Mohammad Rastegari, Munish Bansal, Nandhini Santhanam, Natascha Parks, Natasha White, Navyata Bawa, Nayan Singhal, Nick Egebo, Nicolas Usunier, Nikhil Mehta, Nikolay Pavlovich Laptev, Ning Dong, Norman Cheng, Oleg Chernoguz, Olivia Hart, Omkar Salpekar, Ozlem Kalinli, Parkin Kent, Parth Parekh, Paul Saab, Pavan Balaji, Pedro Rittner, Philip Bontrager, Pierre Roux, Piotr Dollar, Polina Zvyagina, Prashant Ratanchandani, Pritish Yuvraj, Qian Liang, Rachad Alao, Rachel Rodriguez, Rafi Ayub, Raghotham Murthy, Raghu Nayani, Rahul Mitra, Rangaprabhu Parthasarathy, Raymond Li, Rebekkah Hogan, Robin Battey, Rocky Wang, Russ Howes, Ruty Rinott, Sachin Mehta, Sachin Siby, Sai Jayesh Bondu, Samyak Datta, Sara Chugh, Sara Hunt, Sargun Dhillon, Sasha Sidorov, Satadru Pan, Saurabh Mahajan, Saurabh Verma, Seiji Yamamoto, Sharadh Ramaswamy, Shaun Lindsay, Shaun Lindsay, Sheng Feng, Shenghao Lin, Shengxin Cindy Zha, Shishir Patil, Shiva Shankar, Shuqiang Zhang, Shuqiang Zhang, Sinong Wang, Sneha Agarwal, Soji Sajuyigbe, Soumith Chintala, Stephanie Max, Stephen Chen, Steve Kehoe, Steve Satterfield, Sudarshan Govindaprasad, Sumit Gupta, Summer Deng, Sungmin Cho, Sunny Virk, Suraj Subramanian, Sy Choudhury, Sydney Goldman, Tal Remez, Tamar Glaser, Tamara Best, Thilo Koehler, Thomas Robinson, Tianhe Li, Tianjun Zhang, Tim Matthews, Timothy Chou, Tzook Shaked, Varun Vontimitta, Victoria Ajayi, Victoria Montanez, Vijai Mohan, Vinay Satish Kumar, Vishal Mangla, Vlad Ionescu, Vlad Poenaru, Vlad Tiberiu Mihailescu, Vladimir Ivanov, Wei Li, Wenchen Wang, Wenwen Jiang, Wes Bouaziz, Will Constable, Xiaocheng Tang, Xiaojian Wu, Xiaolan Wang, Xilun Wu, Xinbo Gao, Yaniv Kleinman, Yanjun Chen, Ye Hu, Ye Jia, Ye Qi, Yenda Li, Yilin Zhang, Ying Zhang, Yossi Adi, Youngjin Nam, Yu, Wang, Yu Zhao, Yuchen Hao, Yundi Qian, Yunlu Li, Yuzi He, Zach Rait, Zachary DeVito, Zef Rosnbrick, Zhaoduo Wen, Zhenyu Yang, Zhiwei Zhao, and Zhiyu Ma. The llama 3 herd of models, 2024.

[17] Kristen Grauman, Andrew Westbury, Eugene Byrne, Zachary Chavis, Antonino Furnari, Rohit Girdhar, Jackson Hamburger, Hao Jiang, Miao Liu, Xingyu Liu, Miguel Martin, Tushar Nagarajan, Ilija Radosavovic, Santhosh Kumar Ramakrishnan, Fiona Ryan, Jayant Sharma, Michael Wray, Mengmeng Xu, Eric Zhongcong Xu, Chen Zhao, Siddhant Bansal, Dhruv Batra, Vincent Cartillier, Sean Crane, Tien Do, Morrie Doulaty, Akshay Erapalli, Christoph Feichtenhofer, Adriano Fragomeni, Qichen Fu, Abrham Gebreselasie, Cristina Gonzalez, James Hillis, Xuhua Huang, Yifei Huang, Wenqi Jia, Weslie Khoo, Jachym Kolar, Satwik Kottur, Anurag Kumar, Federico Landini, Chao Li, Yanghao Li, Zhenqiang Li, Karttikeya Mangalam, Raghava Modhugu, Jonathan Munro, Tullie Murrell, Takumi Nishiyasu, Will Price, Paola Ruiz Puentes, Merey Ramazanova, Leda Sari, Kiran Somasundaram, Audrey Southerland, Yusuke Sugano, Ruijie Tao, Minh Vo, Yuchen Wang, Xindi Wu, Takuma Yagi, Ziwei Zhao, Yunyi Zhu, Pablo Arbelaez, David Crandall, Dima Damen, Giovanni Maria Farinella, Christian Fuegen, Bernard Ghanem, Vamsi Krishna Ithapu, C. V. Jawahar, Hanbyul Joo, Kris Kitani, Haizhou Li, Richard Newcombe, Aude Oliva, Hyun Soo Park, James M. Rehg, Yoichi Sato, Jianbo Shi, Mike Zheng Shou, Antonio Torralba, Lorenzo Torresani, Mingfei Yan, and Jitendra Malik. Ego4d: Around the world in 3,000 hours of egocentric video, 2022.

[18] Kristen Grauman, Andrew Westbury, Lorenzo Torresani, Kris Kitani, Jitendra Malik, Triantafyllos Afouras, Kumar Ashutosh, Vijay Baiyya, Siddhant Bansal, Bikram Boote, Eugene Byrne, Zach Chavis, Joya Chen, Feng Cheng, Fu-Jen Chu, Sean Crane, Jing Dong, Maria Escobar, Cristhian Forigua, Abrham Gebreselasie, Jing Huang, Mohaiminul Islam, Suyog Jain, Rawal Khirodkar, Kevin J Liang, Jia-Wei Liu, Sagnik Majumder, Yongsen Mao, Miguel Martin, Effrosyni Mavroudi, Tushar Nagarajan, Francesco Ragusa, Santhosh Ramakrishnan, Arjun Somayazulu, Yale Song, Shan Su, Zihui Xue, Edward Zhang, Angela Castillo, Changan Chen, Xinzhu Fu, Ryosuke Furuta, Cristina Gonzalez, Prince Gupta, Jiabo Hu, Yifei Huang, Yiming Huang, Weslie Khoo, Anush Kumar, Sach Lakhavani, Miao Liu, Mi Luo, Zhengyi Luo, Brighid Meredith, Austin Miller, Oluwatumininu Oguntola, Xiaqing Pan, Penny Peng, Shraman Pramanick, Merey Ramazanova, Fiona Ryan, Wei Shan, Kiran Somasundaram, Chenan Song, Audrey Southerland, Huiyu Wang, Yuchen Wang, Takuma Yagi, Mingfei Yan, Xitong Yang, Zecheng Yu, Shengxin Cindy Zha, Chen Zhao, Ziwei Zhao, Zhifan Zhu, Jeff Zhuo, Pablo Arbelaez, Gedas Bertasius, David Crandall, Dima Damen, Jakob Engel, Giovanni Maria Farinella, Antonino Furnari, Bernard Ghanem,

Judy Hoffman, C V Jawahar, Richard Newcombe, Hyun Soo Park, James M Rehg, Yoichi Sato, Manolis Savva, Jianbo Shi, Mike Zheng, and Michael Wray. Ego-exo4d: Understanding skilled human activity from first- and third-person perspectives.

[19] Matthew Honnibal, Ines Montani, Sofie Van Landeghem, and Adriane Boyd. spaCy: Industrial-strength Natural Language Processing in Python. 2020.

[20] Edward J. Hu, Yelong Shen, Phillip Wallis, Zeyuan Allen-Zhu, Yuanzhi Li, Shean Wang, Lu Wang, and Weizhu Chen. Lora: Low-rank adaptation of large language models, 2021.

[21] Shuhei Kurita, Naoki Katsura, and Eri Onami. Refego: Referring expression comprehension dataset from first-person perception of ego4d, 2023.

[22] Jie Lei, Linjie Li, Luowei Zhou, Zhe Gan, Tamara L. Berg, Mohit Bansal, and Jingjing Liu. Less is more: Clipbert for video-and-language learning via sparse sampling, 2021.

[23] Bo Li, Yuanhan Zhang, Dong Guo, Renrui Zhang, Feng Li, Hao Zhang, Kaichen Zhang, Peiyuan Zhang, Yanwei Li, Ziwei Liu, and Chunyuan Li. Llava-onevision: Easy visual task transfer, 2024.

[24] Feng Li, Renrui Zhang, Hao Zhang, Yuanhan Zhang, Bo Li, Wei Li, Zejun Ma, and Chunyuan Li. Llava-next-interleave: Tackling multi-image, video, and 3d in large multimodal models, 2024.

[25] Yanghao Li, Tushar Nagarajan, Bo Xiong, and Kristen Grauman. Ego-exo: Transferring visual representations from third-person to first-person videos, 2021.

[26] Yifei Li, Junbo Niu, Ziyang Miao, Chunjiang Ge, Yuanhang Zhou, Qihao He, Xiaoyi Dong, Haodong Duan, Shuangrui Ding, Rui Qian, Pan Zhang, Yuhang Zang, Yuhang Cao, Conghui He, and Jiaqi Wang. Ovo-bench: How far is your video-llms from real-world online video understanding?, 2025.

[27] Junming Lin, Zheng Fang, Chi Chen, Zihao Wan, Fuwen Luo, Peng Li, Yang Liu, and Maosong Sun. StreamingBench: Assessing the gap for MLLMs to achieve streaming video understanding. In *None*, 2024.

[28] Kevin Qinghong Lin, Alex Jinpeng Wang, Mattia Soldan, Michael Wray, Rui Yan, Eric Zhongcong Xu, Difei Gao, Rongcheng Tu, Wenzhe Zhao, Weijie Kong, Chengfei Cai, Hongfa Wang, Dima Damen, Bernard Ghanem, Wei Liu, and Mike Zheng Shou. Egocentric video-language pretraining, 2022.

[29] Xiangrui Liu, Yan Shu, Zheng Liu, Ao Li, Yang Tian, and Bo Zhao. Video-xl-pro: Reconstructive token compression for extremely long video understanding, 2025.

[30] Karttikeya Mangalam, Raiymbek Akshulakov, and Jitendra Malik. Egoschema: A diagnostic benchmark for very long-form video language understanding, 2023.

[31] Zaira Manigrasso, Matteo Dunnhofer, Antonino Furnari, Moritz Nottebaum, Antonio Finocchiaro, Davide Marana, G. Farinella, and C. Micheloni. Online episodic memory visual query localization with egocentric streaming object memory.

[32] Xavi Puig, Eric Undersander, Andrew Szot, Mikael Dallaire Cote, Ruslan Partsey, Jimmy Yang, Ruta Desai, Alexander William Clegg, Michal Hlavac, Tiffany Min, Theo Gervet, Vladimir Vondrus, Vincent-Pierre Berges, John Turner, Oleksandr Maksymets, Zsolt Kira, Mrinal Kalakrishnan, Jitendra Malik, Devendra Singh Chaplot, Unnat Jain, Dhruv Batra, Akshara Rai, and Roozbeh Mottaghi. Habitat 3.0: A co-habitat for humans, avatars and robots, 2023.

[33] Rui Qian, Shuangrui Ding, Xiaoyi Dong, Pan Zhang, Yuhang Zang, Yuhang Cao, Dahua Lin, and Jiaqi Wang. Dispider: Enabling video llms with active real-time interaction via disentangled perception, decision, and reaction, 2025.

[34] Rui Qian, Xiaoyi Dong, Pan Zhang, Yuhang Zang, Shuangrui Ding, Dahua Lin, and Jiaqi Wang. Streaming long video understanding with large language models, 2024.

[35] Lu Qiu, Yi Chen, Yuying Ge, Yixiao Ge, Ying Shan, and Xihui Liu. Egoplan-bench2: A benchmark for multimodal large language model planning in real-world scenarios, 2025.

[36] Alec Radford, Jong Wook Kim, Chris Hallacy, Aditya Ramesh, Gabriel Goh, Sandhini Agarwal, Girish Sastry, Amanda Askell, Pamela Mishkin, Jack Clark, Gretchen Krueger, and Ilya Sutskever. Learning transferable visual models from natural language supervision, 2021.

[37] Shuhuai Ren, Linli Yao, Shicheng Li, Xu Sun, and Lu Hou. Timechat: A time-sensitive multimodal large language model for long video understanding, 2024.

[38] Ivan Rodin, Antonino Furnari, Kyle Min, Subarna Tripathi, and Giovanni Maria Farinella. Action scene graphs for long-form understanding of egocentric videos, 2023.

[39] Michael S. Ryoo, Honglu Zhou, Shrikant Kendre, Can Qin, Le Xue, Manli Shu, Jongwoo Park, Kanchana Ranasinghe, Silvio Savarese, Ran Xu, Caiming Xiong, and Juan Carlos Niebles. xgen-mm-vid (blip-3-video): You only need 32 tokens to represent a video even in vlms, 2025.

[40] Manolis Savva, Abhishek Kadian, Oleksandr Maksymets, Yili Zhao, Erik Wijmans, Bhavana Jain, Julian Straub, Jia Liu, Vladlen Koltun, Jitendra Malik, Devi Parikh, and Dhruv Batra. Habitat: A Platform for Embodied AI Research. In *Proceedings of the IEEE/CVF International Conference on Computer Vision (ICCV)*, 2019.

[41] Yuhan Shen, Huiyu Wang, Xitong Yang, Matt Feiszli, Ehsan Elhamifar, Lorenzo Torresani, and Effrosyni Mavroudi. Learning to segment referred objects from narrated egocentric videos. In *2024 IEEE/CVF Conference on Computer Vision and Pattern Recognition (CVPR)*, pages 14510–14520. IEEE.

[42] Cheng Shi, Yizhou Yu, and Sibei Yang. Vision function layer in multimodal llms, 2025.

[43] Yan Shu, Zheng Liu, Peitian Zhang, Minghao Qin, Junjie Zhou, Zhengyang Liang, Tiejun Huang, and Bo Zhao. Video-xl: Extra-long vision language model for hour-scale video understanding, 2024.

[44] Yale Song, Gene Byrne, Tushar Nagarajan, Huiyu Wang, Miguel Martin, and Lorenzo Torresani. Ego4d goal-step: Toward hierarchical understanding of procedural activities. In *Thirty-seventh Conference on Neural Information Processing Systems Datasets and Benchmarks Track*, 2023.

[45] Andrew Szot, Alex Clegg, Eric Undersander, Erik Wijmans, Yili Zhao, John Turner, Noah Maestre, Mustafa Mukadam, Devendra Chaplot, Oleksandr Maksymets, Aaron Gokaslan, Vladimir Vondrus, Sameer Dharur, Franziska Meier, Wojciech Galuba, Angel Chang, Zsolt Kira, Vladlen Koltun, Jitendra Malik, Manolis Savva, and Dhruv Batra. Habitat 2.0: Training home assistants to rearrange their habitat. In *Advances in Neural Information Processing Systems (NeurIPS)*, 2021.

[46] Yansong Tang, Dajun Ding, Yongming Rao, Yu Zheng, Danyang Zhang, Lili Zhao, Jiwen Lu, and Jie Zhou. Coin: A large-scale dataset for comprehensive instructional video analysis, 2019.

[47] Hugo Touvron, Thibaut Lavril, Gautier Izacard, Xavier Martinet, Marie-Anne Lachaux, Timothée Lacroix, Baptiste Rozière, Naman Goyal, Eric Hambro, Faisal Azhar, Aurelien Rodriguez, Armand Joulin, Edouard Grave, and Guillaume Lample. Llama: Open and efficient foundation language models, 2023.

[48] Ashish Vaswani, Noam Shazeer, Niki Parmar, Jakob Uszkoreit, Llion Jones, Aidan N. Gomez, Lukasz Kaiser, and Illia Polosukhin. Attention is all you need, 2023.

[49] Peng Wang, Shuai Bai, Sinan Tan, Shijie Wang, Zhihao Fan, Jinze Bai, Keqin Chen, Xuejing Liu, Jialin Wang, Wenbin Ge, Yang Fan, Kai Dang, Mengfei Du, Xuancheng Ren, Rui Men, Dayiheng Liu, Chang Zhou, Jingren Zhou, and Junyang Lin. Qwen2-vl: Enhancing vision-language model's perception of the world at any resolution, 2024.

[50] Weihan Wang, Zehai He, Wenyi Hong, Yean Cheng, Xiaohan Zhang, Ji Qi, Xiaotao Gu, Shiyu Huang, Bin Xu, Yuxiao Dong, Ming Ding, and Jie Tang. Lvbench: An extreme long video understanding benchmark, 2025.

[51] Yueqian Wang, Xiaojun Meng, Yuxuan Wang, Jianxin Liang, Jiansheng Wei, Huishuai Zhang, and Dongyan Zhao. Videollm knows when to speak: Enhancing time-sensitive video comprehension with video-text duet interaction format, 2024.

[52] Shiwei Wu, Joya Chen, Kevin Qinghong Lin, Qimeng Wang, Yan Gao, Qianli Xu, Tong Xu, Yao Hu, Enhong Chen, and Mike Zheng Shou. Videollm-mod: Efficient video-language streaming with mixture-of-depths vision computation, 2024.

[53] Guangxuan Xiao, Yuandong Tian, Beidi Chen, Song Han, and Mike Lewis. Efficient streaming language models with attention sinks, 2024.

[54] Jingkang Yang, Shuai Liu, Hongming Guo, Yuhao Dong, Xiamengwei Zhang, Sicheng Zhang, Pengyun Wang, Zitang Zhou, Binzhu Xie, Ziyue Wang, Bei Ouyang, Zhengyu Lin, Marco Cominelli, Zhongang Cai, Yuanhan Zhang, Peiyuan Zhang, Fangzhou Hong, Joerg Widmer, Francesco Gringoli, Lei Yang, Bo Li, and Ziwei Liu. Egolife: Towards egocentric life assistant, 2025.

[55] Xitong Yang, Fu-Jen Chu, Matt Feiszli, Raghav Goyal, Lorenzo Torresani, and Du Tran. Relational space-time query in long-form videos. In *2023 IEEE/CVF Conference on Computer Vision and Pattern Recognition (CVPR)*, pages 6398–6408. IEEE.

[56] Yuan Yao, Tianyu Yu, Ao Zhang, Chongyi Wang, Junbo Cui, Hongji Zhu, Tianchi Cai, Haoyu Li, Weilin Zhao, Zhihui He, Qianyu Chen, Huarong Zhou, Zhensheng Zou, Haoye Zhang, Shengding Hu, Zhi Zheng, Jie Zhou, Jie Cai, Xu Han, Guoyang Zeng, Dahai Li, Zhiyuan Liu, and Maosong Sun. Minicpm-v: A gpt-4v level mllm on your phone, 2024.

[57] Hanrong Ye, Haotian Zhang, Erik Daxberger, Lin Chen, Zongyu Lin, Yanghao Li, Bowen Zhang, Haoxuan You, Dan Xu, Zhe Gan, Jiasen Lu, and Yinfei Yang. Mm-ego: Towards building egocentric multimodal llms for video qa, 2025.

[58] Xubing Ye, Yukang Gan, Xiaoke Huang, Yixiao Ge, and Yansong Tang. Voco-llama: Towards vision compression with large language models, 2025.

[59] Gokul Yenduri, Ramalingam M, Chemmalar Selvi G, Supriya Y, Gautam Srivastava, Praveen Kumar Reddy Maddikunta, Deepti Raj G, Rutvij H Jhaveri, Prabadevi B, Weizheng Wang, Athanasios V. Vasilakos, and Thippa Reddy Gadekallu. Generative pre-trained transformer: A comprehensive review on enabling technologies, potential applications, emerging challenges, and future directions, 2023.

[60] Xiaohua Zhai, Basil Mustafa, Alexander Kolesnikov, and Lucas Beyer. Sigmoid loss for language image pre-training, 2023.

[61] Haoji Zhang, Yiqin Wang, Yansong Tang, Yong Liu, Jiashi Feng, Jifeng Dai, and Xiaojie Jin. Flash-vstream: Memory-based real-time understanding for long video streams, 2024.

[62] Jiahao Zhang, Stephen Gould, and Itzik Ben-Shabat. Vidat—ANU CVML video annotation tool. https://github.com/anucvml/vidat, 2020.

[63] Peitian Zhang, Zheng Liu, Shitao Xiao, Ninglu Shao, Qiwei Ye, and Zhicheng Dou. Long context compression with activation beacon, 2024.

[64] Yue Zhao, Ishan Misra, Philipp Krähenbühl, and Rohit Girdhar. Learning video representations from large language models, 2022.

[65] Ge Zheng, Bin Yang, Jiajin Tang, Hong-Yu Zhou, and Sibei Yang. Ddcot: Duty-distinct chain-of-thought prompting for multimodal reasoning in language models, 2023.

[66] Junjie Zhou, Yan Shu, Bo Zhao, Boya Wu, Zhengyang Liang, Shitao Xiao, Minghao Qin, Xi Yang, Yongping Xiong, Bo Zhang, Tiejun Huang, and Zheng Liu. Mlvu: Benchmarking multi-task long video understanding, 2025.